Engineering Novel Microbead Encapsulated Three-Dimensional Tumor and Stem Cell Models

by

Tanya Nanda

A Thesis Presented in Partial Fulfillment
of the Requirements for the Degree
Master of Science

Approved November 2020 by the
Graduate Supervisory Committee:

Kaushal Rege, Chair
Jennifer Blain Christen
Jessica Weaver

ARIZONA STATE UNIVERSITY

December 2020

ABSTRACT

Cellular assays are the backbone of biological studies - be it for tissue modeling, drug discovery, therapeutics, or diagnostics. Two-dimensional (2D) cell culture has been deployed for several decades to garner physiologically relevant information and predict data before the cost-intensive animal testing. Although 2D techniques have been valuable for cellular assays, they have a colossal limitation - they do not adequately consider the natural three-dimensional (3D) microenvironment of the cells. As a result, they sometimes provide misleading statistics. Therefore, it is important to develop a 3D model that predicts cellular behaviors and their interaction with neighboring cells and extracellular matrix (ECM) in a more realistic manner. In recent biomedical research, various platforms have been modeled to generate 3D prototypes of tissues, *spheroids*, in vitro that could allow the study of cellular responses resembling in vivo environments, such as matrices, scaffolds, and devices. But most of these platforms have drawbacks such as lack of spheroid size control, low yield, or high cost associated with them. On the other hand, Amikagel is a low cost, high-fidelity platform that can facilitate the convenient generation of tumor and stem cell spheroids. Furthermore, Amikabeads are aminoglycoside-derived hydrogel microbeads derived from the same monomers as Amikagel. They are a versatile platform with several chemical groups that can be exploited for encapsulating the spheroids and investigating the delivery of bioactive compounds to the cells. This thesis is focused on engineering novel 3D tumor and stem cell models generated on Amikagel and encapsulated in Amikabeads for proximal delivery of bioactive compounds and applications in regenerative medicine.

To Dad,

I hope you are happy wherever you are.

To Mom, Karan, and Dollar,

Thank you for teaching me about dreams and for your unwavering faith in me while I was busy catching them.

ACKNOWLEDGMENTS

First and foremost, for all that I have achieved during my academic journey at Arizona State, I would like to thank Dr. Kaushal Rege for constant encouragement and guidance. His invaluable insights helped formulate and shape an idea into this thesis. I learnt about the perspective and self-criticism one needs to have to approach scientific roadblocks and tackle them, which was way more valuable than technical skills. I highly appreciate his moral support and instrumental feedback about my personal and academic goals. Next, I would like to massively thank my supervisor and doctoral researcher, Rajesh, for teaching me the ways of academic research and beyond. He was beside me every step of the way and his support led me to be chosen for five research grants and two assistantships, which I am indebted for. I would also like to thank members of the Rege Bioengineering Laboratory – Dr. Jordan Yaron for his help with the histology studies and Mr. Subhadeep Dutta for providing Amikabeads and contributing to this project and my growth. I am also grateful to Dr. Alexandra Lucas for letting me use the histology equipment and microscope for parts of my research. In addition, I would like to thank my committee members, Dr. Blain Christen and Dr. Weaver for their guidance as I conducted this research. It was an honor to have them on my thesis committee.

For financial support, I would like to thank Dr. Rege and the National Institutes of Health; Master's Opportunity for Research in Engineering (MORE) award from ASU; Graduate Research Support Program from Graduate and Professional Student Association (GPSA) and The Graduate College, ASU; and Kern Entrepreneurial Engineering Network (KEEN) award from ASU Kern Project.

My passion for biomedicine and healthcare research has stemmed from my mother, who is a force of nature. I am grateful to her and my brother for teaching me all the right things. They are my biggest pillars of strength and this thesis would not have been possible without their support. Having lost my father to a cancer battle, I was lost for a long time and this research is a way of giving him back for everything he did for me. I would also like to mention Dollar, my beloved dog, for making me smile from miles away on the hardest of the days. I want to extend a massive thank you to my support system in Arizona, my home away from home – Pralak and Anindya – for keeping me sane through these two intense years. I cannot express in words how much their love and comfort meant to me.

TABLE OF CONTENTS

Page

LIST OF TABLES viii

LIST OF FIGURES ix

CHAPTER

1 INTRODUCTION 1

1.1 Two-Dimensional Cell Culture 1

1.2 Need for Three-Dimensional Cell Culture 2

1.3 Biology of 3D Cell Culture 3

1.4 Platforms for 3D Cell Culture 6

1.5 Amikagel Technology 12

1.6 3D Encapsulated Models 14

1.7 Amikabeads – A Hydrogel Microbead Platform 18

1.8 3D Models in Regenerative Medicine and Tissue Engineering 19

1.9 Overview 21

2 MATERIALS AND METHODS 23

2.1 Amikagel Preparation 23

2.2 Generation of Amikagel Coated Cell-Culture Plates 24

2.3 Cell Culture 24

2.4 Generation of 3D Spheroids 25

2.5 Preparation of Parental Amikabeads 25

2.6 Preparation of Quaternized Amikabeads 26

2.7 Ninhydrin Assay 27

CHAPTER Page

2.8 Encapsulation of Spheroids 27

2.9 Conjugation of Amikabeads with Rhodamine 28

2.10 Conjugation of Amikabeads with Fluorescein..... 28

2.11 Encapsulation of Spheroids in Rho-Conjugated Amikabeads 29

2.12 Encapsulation of Spheroids in Fluorescein-Conjugated Amikabeads 30

2.13 Fluorescence Intensity Optimization 31

2.14 Fluorescence Labeling of Spheroids 32

2.15 Phase Contrast Microscopy 34

2.16 Laser-Scanning Confocal Microscopy 34

2.17 Confocal Microscopy with Dipping Objective Lens 35

2.18 Viability Assays..... 35

2.19 Flow Cytometry 36

3 RESULTS AND DISCUSSION 37

3.1 Amikagel Coated Cell Culture Plates 37

3.2 Formation of Spheroids 35

3.3 Amikabeads Synthesis..... 41

3.4 Amikabeads Characterization 41

3.5 Quaternization of Amikabeads..... 43

3.6 Amikabeads-Encapsulated Spheroids 44

3.7 Low Speed Centrifugation Enhances Encapsulation 50

3.8 Fluorescent-Tag Labeled Amikabeads..... 52

3.9 Fluorescence Intensity Optimization..... 53

CHAPTER Page

3.10 Visualization of Encapsulated Tumor Models 55

3.11 Visualization of Encapsulated hMSC Models 63

3.12 Cell Viability Assay 72

3.13 Flow Cytometry 73

4 CONCLUSIONS 75

5 FUTURE DIRECTIONS 76

REFERENCES 78

LIST OF TABLES

Table		Page
1.	Materials for Scaffold Generation	6
2.	Spheroid Generation Methods	10
3.	Comparison of Spheroid Generation Platforms	13
4.	Amikagel Compositions	23
5.	Rho-conjugated Amikabeads	29
6.	Fluorescein-conjugated Amikabeads	31
7.	Spheroid Stains	33
8.	Spheroid Formation	39
9.	Fluorescence Intensity	54

LIST OF FIGURES

Figure		Page
1.	Conventional Monolayer Cell Culture	1
2.	3D Cell Culture	3
3.	Spheroid Formation Model	4
4.	Spheroid Microenvironment.	5
5.	Methods for 3D Multicellular Spheroid Formation	9
6.	Generation of 3D Tumor Microenvironments (3DTM) On Amikagel	12
7.	Encapsulation of Spheroids	16
8.	Plasma Membrane of Cells	19
9.	Application of Spheroids in Tissue Repair and Regeneration.	20
10.	Clinical Significance of MSC Spheroids.	21
11.	Amikagel Formation.	38
12.	Spheroid Generation	40
13.	Synthesis of Amikabeads.	42
14.	Characterization of Amikabeads	42
15.	Ninhydrin Assay	43
16.	Amikabeads-Encapsulated Spheroid	45
17.	Amikacin	46
18.	Amikabeads-Encapsulated T-47D Spheroids.	47
19.	Interspersed Region Between Spheroid and Amikabeads	48
20.	Spheroid Encapsulation Using Centrifugation.	50

Figure Page

21. Rho-Conjugated Amikabeads. 52

22. Fluorescein-Conjugated Amikabeads. 53

23. Intensity Optimization of Fluorescein-Conjugated Amikabeads. 54

24. Fluorescence Microscopy Images of Encapsulated T-47D Spheroid. 56

25. Z-Stack Projection of Encapsulated T-47D Spheroid. 58

26. 3D Projections Of Z-Stacks of Encapsulated T-47D Spheroids 59

27. Confocal Microscopy Images of Encapsulated A375 Spheroids. 61

28. Confocal Microscopy Images of Encapsulated A375 Spheroids. 63

29. Dipping Lens Confocal Microscopy of Encapsulated A375 Spheroids 64

30. Encapsulated hMSC Spheroids 67

31. Encapsulated hMSC Spheroids. 70

32. Cell Viability Assay. 72

33. Proximal Delivery of Bioactive Compounds. 76

34. Multicellular Construct Using Spheroid and Amikabeads. 77

CHAPTER 1

INTRODUCTION

1.1 Two-Dimensional Cell Culture

The technique of cell culture was developed by Harrison in 1907 while studying the nerve fiber origin.[1] The process demonstrated a way to maintain cells outside the body of origin and study them over a longer period. Over the years, substantial improvement has been made such as the cell culture flasks used to grow cells with ease, use of cheap, easy to-produce synthetic medium, and addition of antibiotics to avoid bacterial and fungal contaminations.

Traditional two-dimensional (2D) culture systems involve cells growing in monolayers on flat solid surfaces, potentially polystyrene cell culture flasks or plates, with synthetic medium as the source of nutrition at body temperature (37°C) as illustrated in **Fig. 1**.

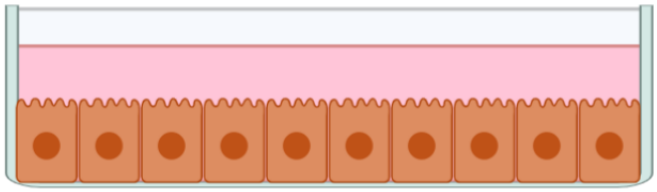


Fig. 1. Conventional monolayer cell culture. The cells grow flat on a solid surface such as a cell culture flask or a plate, supplemented by nutrient media (in pink). *(Created with BioRender.com)*

Supplements such as Fetal Bovine Serum and L-Glutamine are commonly used to catalyze the growth of cells. Cells are sub-cultured (or passaged) frequently, depending upon the cell line, to prevent necrosis due to nutrient exhaustion. The cells are removed from the

culture dish surface using Trypsin-EDTA (0.25%) and a diluted aliquot from the stock culture is reseeded into a flask to continue the cell line.[2]

Although this technique has been routinely used as the basis of cell culture and a screening model to precede preclinical studies for quite a while, it fails to imitate the intracellular or cell-matrix interactions that are present in cells in vivo.[3] Amongst other things, the architecture, morphology, signal transduction, and differentiation are the aspects of cell culture that are lost in this standard technique and have been questioned.[2,4,5]

1.2 Need for Three-Dimensional Cell Culture

These limitations call for an alternative method of mimicking the cell phenotype outside the organism. Cells in vivo are in three-dimensional (3D) microenvironment consisting of biophysical and biomechanical signaling that is responsible for cellular functions such as migration, adhesion, and proliferation.[6–9] Cellular processes essential for tissue engineering such as differentiation and morphogenesis of cells have also been known to occur preferentially in 3D instead of 2D.[9,10] These 3D in vitro models are on the crossroads between cell biology and tissue engineering due to their multidimensional architecture. They can prove to be potentially successful prototypes of highly expensive and time-consuming animal studies and therefore, bridge the gap between them and monolayer cultures.[3] Such a model predicting cellular behaviors could guide researchers to reject hypotheses at an earlier stage of the study (**Fig. 2**).

Subsequently, 3D cell culture has recently become the point of interest for biology research to improve these simulations of cell microenvironments in vitro.[11] For instance, pluripotent stem cells from brains can be used to generate 3D organoids, called neural organoids or brain assembloids.[12,13] Furthermore, cells in 3D culture have also demonstrated increased resistivity to certain chemotherapeutic drugs, indicating towards the potential dormancy of cells in 3D.[14]

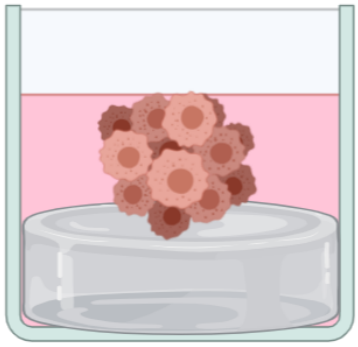


Fig. 2. 3D cell culture. Due to lack of adhesivity to the surface, the intracellular contact increases and the cells grow in a 3D form. *(Created with BioRender.com)*

Such studies conveying the importance of 3D culture are the motivation for this project. It aims to investigate the potential to generate 3D tumor and stem cell models and their possibility of application in regenerative medicine and drug discovery.

1.3 Biology of 3D Cell Culture

As reported in the literature, it is essential to preserve the natural features and architecture of tissues while culturing their functional units (cells) in 3D.[15] The most common way to culture cells in 3D is making use of modified cell culture surfaces to prevent cell adhesion

and thus, promote 3D culture formation. These culture techniques give rise to spherical multicellular aggregates known as ***spheroids*.**

As illustrated in **Fig. 3**, complex cell adhesion and differentiation are the primary contributing factors in spheroid formation, which is a three-step process:[16]

1. Loose cell aggregates are generated via integrin-ECM binding.
2. A period of delay for cadherin expression and accumulation.
3. Compact spheroids are generated through homophilic cadherin-cadherin interactions.

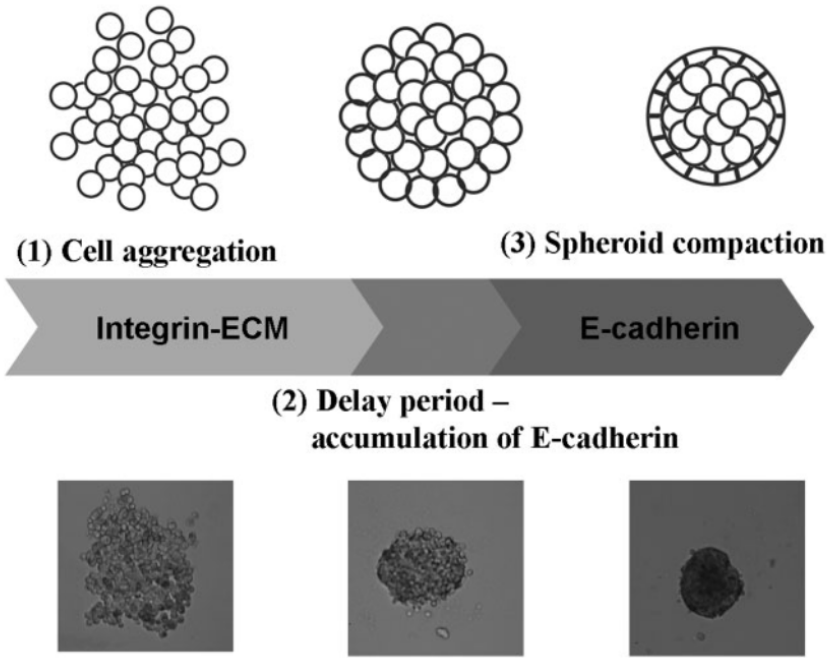


Fig. 3. Spheroid formation model. Spheroid formation can be divided into three stages: (1) Cell aggregation, (2) Delay period, and (3) Spheroid compaction.[1]

[1] Reprinted (adapted) with permission from Lin, R.-Z., Lin, R.-Z. & Chang, H.-Y. Recent advances in three-dimensional multicellular spheroid culture for biomedical research. *Biotechnol J* **3**, 1172–1184 (2008).

Along with spheroid formation models, several reports have been published proposing mathematical models to stimulate the movement of nutrients, oxygen, and waste transport in and out of the spheroid.[17–19] As demonstrated in **Fig. 4**, it has been reported that spheroids resemble avascular tissues with diffusion limitations of 150-200 μm to many molecules, including O_2. Because of waste accumulation inside them, spheroids with diameters greater than 500 μm display layered structures comprising a necrotic core, surrounded by a rim of viable cells.[17,20,21]

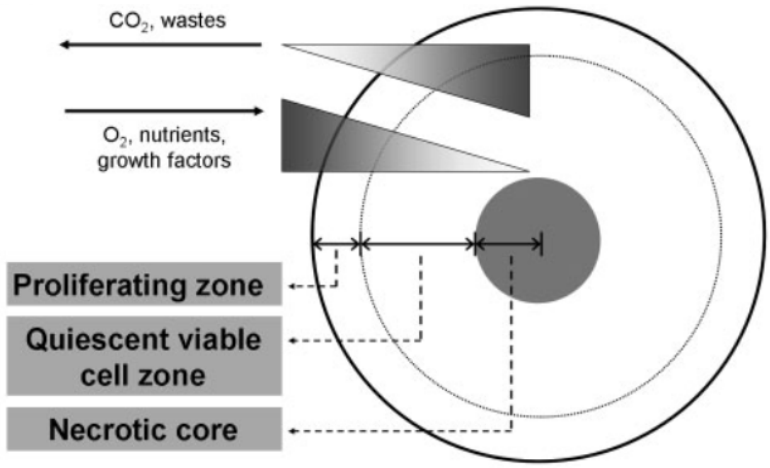


Fig. 4. Spheroid microenvironment. Tumor spheroids are spherical with a concentric geometry of proliferating, quiescent, and dead cells. An insufficient mass transport through the cellular barriers leads to the formation of a necrotic core.[2]

[2] Reprinted (adapted) with permission from Lin, R.-Z., Lin, R.-Z. & Chang, H.-Y. Recent advances in three-dimensional multicellular spheroid culture for biomedical research. *Biotechnol J* **3**, 1172–1184 (2008).

1.4 Platforms for 3D Cell Culture

Unlike 2D, a standard method of operation has not been defined for 3D cell culture. Over the years, several methods have been engineered and reported based upon the nature of cells and the culture applications. Some of them have been illustrated in **Fig. 5** and discussed below.

Scaffolds. Prefabricated scaffolds incorporated with biological cues are most used for culture of spheroids. These scaffolds are typically biocompatible and degrade and resorb at a rate aligning with the tissue growth, thus, defining the shape and function of the 3D culture.[22] Both synthetic and natural materials have been used to generate scaffolds for 3D culture, as mentioned in **Table 1**. While natural materials provide biocompatibility, synthetic materials have a higher mechanical strength. Thus, a combination of both is used.

Table 1. Synthetic and natural materials for 3D culture scaffolds

Materials for Scaffold Generation		
Nature	**Types**	**Advantages**
Natural	Silk, Collagen, Alginate	Biocompatible Mechanical and biological properties similar to in vivo features
Synthetic	PEG, PGA, PLGA, Polystyrene	Mechanically strong Long shelf life Do not interact with cells

Forced-floating method. To avoid the adherence of cells to the vessel surface, they are forced to float using surface modification (**Fig. 5a**) promotes intracellular contact and thus, spheroid formation.[23] This technique allows for easily reproducible and size adjustable spheroids, making it compatible with high throughput drug discovery studies.[24] Although this method is ideal for long term and homogeneous culture of cells, the time and work required for coating the cell culture plates before seeding them is a drawback.

Hanging drop method. As illustrated in **Fig. 5b**, this method is an adaptation of Harrison's 2D cell culture technique.[2] Briefly, it includes pipetting a small aliquot of single cell suspension into a microwell tray which is then inverted. The surface tension causes the drops of cell suspension to hang and cells get collected at their tip. The dops give rise to spheroids and this method is reported to have a 100% yield per drop.[25] Although relatively simple, this method has a limitation of the volume of cell suspension hanging from the drop and the difficulty in changing spent media without disturbing the spheroid.[26]

Spinner flask bioreactors and rotational culture systems. As illustrated in **Fig. 5c**, spinner flask bioreactors hold the cell suspension in a container and ensure continuous agitation using a stirring element.[27] This method offers simple and size tunable spheroids but the cellular physiology might be affected due to the sheer force experience by the cells in the spinner.[23]

On the other hand, rotating cell culture bioreactors use a rotating culture container instead of a stirring element, as demonstrated in **Fig. 5c-ii**. The contents of the container experience less sheer force in this case, which is one of the advantages of this system.[28]

Matrices. Several artificial matrices have also been developed for the generation of 3D cell culture. A commercially available ECM known as Matrigel (BD Biosciences) is commonly used for 3D culture support. Components of basement membrane essential for cell differentiation are added which enable the generation of 3D spheroids.[29] There are various other commercially available matrices used to culture spheroids, but due to the high cost associated with their purchase, they are not the preferred method of 3D culture.

Microfluidic cell culture platforms. As illustrated in **Fig. 5**, microfluidic platforms can also be designed to generate spheroids for high-throughput applications such as drug screening. A system engineered by Tan et al. comprises a primary microfluidic channel with an array of micropillars. Cell suspension is passed through this channel and the micropillar array immobilizes the cells within it to support their growth and enable cell–cell interactions. This is followed by passing collagen matrix which forms a thin, conforming layer over the cells and allowing for cell-matrix interactions.[30]

The proposed advantages and disadvantages of methods of spheroid generation have been discussed in **Table 2.**

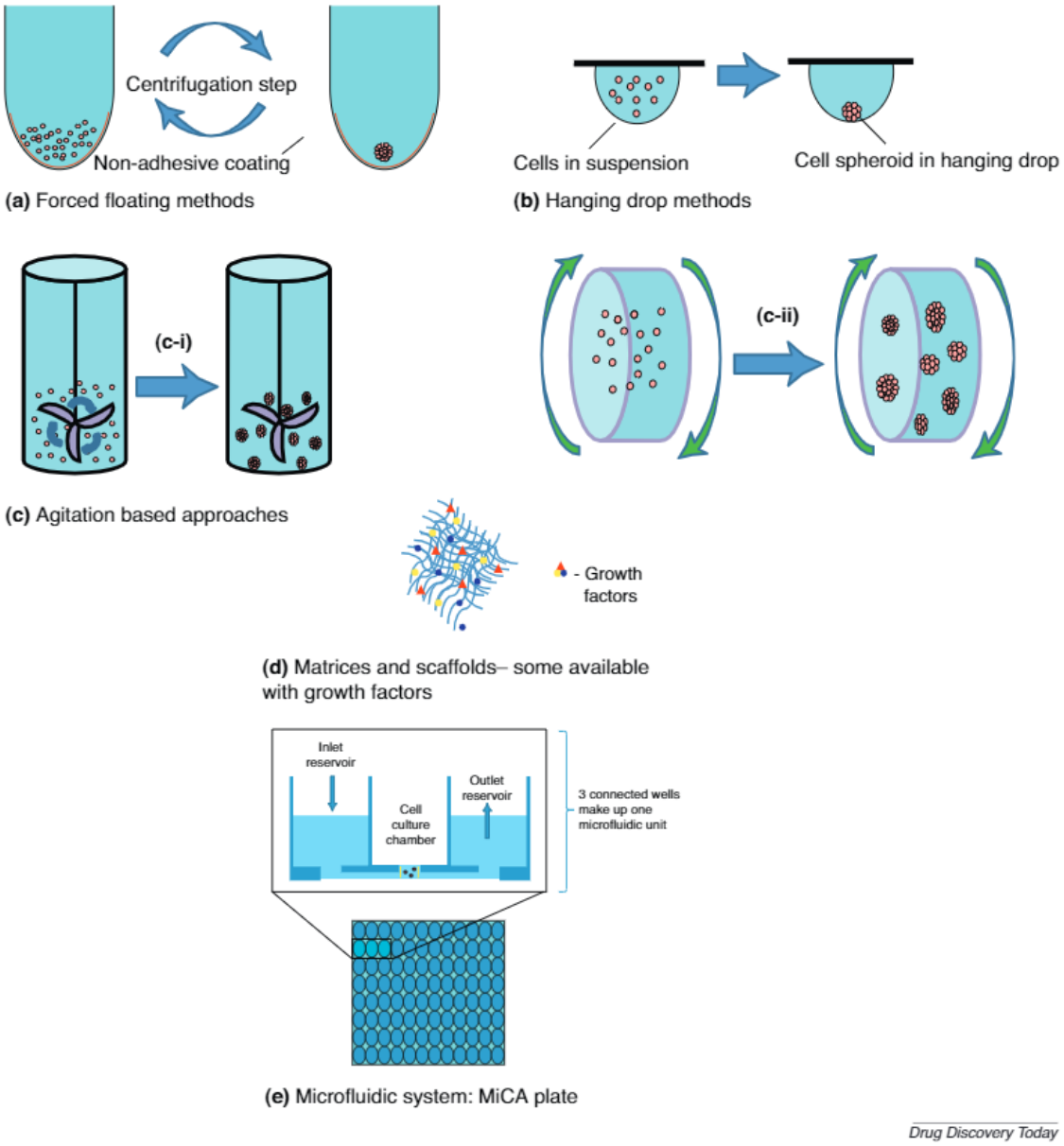


Fig. 5. Methods for 3D multicellular spheroid formation. The methods include (i) forced floating methods, (ii) hanging drop methods, (iii) agitation-based approaches – spinner flask bioreactors and rotational culture systems, and (iv) microfluidic cell culture platforms.[3]

[3] Reprinted from Breslin, S. & O'Driscoll, L. Three-dimensional cell culture: the missing link in drug discovery. Drug *Discov Today* **18**, 240–249, Copyright (2013) with permission from Elsevier.

Table 2. Comparison of spheroid generation methods[4]

Spheroid Generation Methods		
Method Type	**Advantages**	**Disadvantages**
Forced-floating	• Relatively simple • Inexpensive • Suitable for high-throughput testing • Spheroids produced are easily accessible	• Variability in cell size and shape if not as fixed cell no./well • DIY plate-coating is relatively labor intensive
Hanging drop	• Inexpensive if using standard • 96-well plate • Homogenous spheroids suitable for high-throughput testing • Spheroids produced are easily accessible	• More expensive if using specialized plates • Labor intensive if preparing plates in-house • Small culture volume makes medium exchange, without disturbing cells, difficult (proposed easier handling with commercially available formats)

[4] Reprinted from Breslin, S. & O'Driscoll, L. Three-dimensional cell culture: the missing link in drug discovery. Drug *Discov Today* **18**, 240–249, Copyright (2013) with permission from Elsevier.

Agitation-based approaches	• Simple to culture cells • Large-scale production relatively easily achievable • Motion of culture assists nutrient transport • Spheroids produced are easily accessible	• Specialized equipment required • No control over cell no./size of spheroid (can be overcome by additional culture step; see 'Forced-floating methods') • Time consuming due to extra step required for homogenous spheroids • Cells possibly exposed to shear force in spinner flasks (may be problematic for sensitive cells)
Matrices and scaffolds	• Provide 3D support that mimics in vivo • Some incorporate growth factors	• Can be expensive for large-scale production • Can have difficulty in retrieving cells following 3D culture formation
Microfluidic cell culture platforms	• Described as suitable for high-throughput testing	• Specialized equipment required adding expense • Further analysis of 3D cultures produced may be difficult

1.5 Amikagel Technology

Amikagel, a chemomechanically engineered versatile platform for generation of 3D tumor spheroids was reported by Grandhi et al. in 2017 (**Fig. 6**).[31] It is a polymer of amikacin hydrate (AH) and poly(ethylene glycol)diglycidyl ether (PEGDE) and acted as a multipurpose technology to facilitate the identification of different therapeutic approaches for the ablation of spheroids as well as escaped cells.[31]

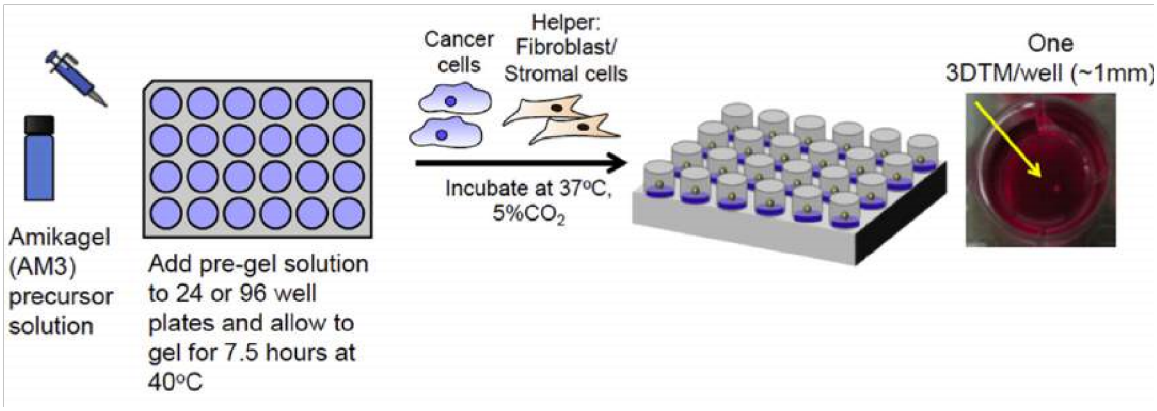


Fig. 6. Generation of 3D Tumor Microenvironments (3DTM) on Amikagel.[5] The 3DTM could be visualized by naked eye, as demonstrated above.

Advantages of Amikagel over 3D spheroid generation platforms. The disadvantages of previously mentioned platforms for 3D spheroid generation gave Amikagel technology an advantage over them for high-throughput, low-cost, and low-effort spheroid generation for this project. The mechanical stiffness and adhesivity of Amikagel played a crucial role in

[5]Reprinted from Grandhi, T. S. P., Potta, T., Nitiyanandan, R., Deshpande, I. & Rege, K. Chemomechanically engineered 3D organotypic platforms of bladder cancer dormancy and reactivation. *Biomaterials* **142**, 171–185, Copyright (2017), with permission from Elsevier.

spheroid formation with 100% yield. No specialized equipment was required to coat the cell culture plates with Amikagel in-house. Changing the media through aspiration was unchallenging and homogeneously sized spheroids were generated. The spheroid size depended on the initial cell density seeded onto the plates. The spheroids were formed within 24-72 hours of seeding. Moreover, this technique is suitable for long-term culture for applications that require media or reagent exchange, unlike non-adherent surfaces such as gel arrays generated from PEG or Corning Ultra-Low Attachment Microplates. Amikagel also shows higher homogeneity in the synthetic cellular microenvironment and can be customized according to the cell line and nature of application by changing the molar ratios of AH and PEGDE. These characteristics put Amikagel one step ahead of the existing technologies for the generation of novel encapsulated models for this research work (as discussed in **Table 3**).

Table 3. Comparison of characteristics of Amikagel with other platforms used for spheroid generation

Comparison of Spheroid Generation Platforms					
Key Characteristics	**Matrices and Scaffolds**	**Forced Floating and Hanging Drop**	**Microfluidic Devices**	**Non-Adherent Surfaces**	**Amikagel**
Support	✓	✗	✓	✓	✓
Convenience	✗	✗	✗	✓	✓

Cost	Variable	✗	✗	✓	✓
Spheroid Yield	Variable	✓	✓	✓	✓
Spheroid Size Homogeneity	✗	✓	✗	✗	✓
Medium Exchange	✓	✗	✓	✗	✓
Accessibility of Spheroids	✗	✓	✗	✓	✓

1.6 3D Encapsulated Models

During this research, optimization was carried out to potentially encapsulate spheroids in a biocompatible material to understand the cellular progression and proximal delivery of bioactive compounds such as small molecules, dyes, and/or drugs to the spheroid. Various encapsulation studies have already been reported using materials such as alginate and collagen. But these techniques involve the use of high cost and complexity equipment such as microfluidic devices and 3D bioprinters.

Recently, cellular capsules have been used as a substitute tool for spheroid encapsulation and study of tumor progression in vivo.[32] The capsules consisted of encapsulating tens of cells (WT mouse colon carcinoma CT26, HeLa, and mouse sarcoma S180 cell lines) in an aqueous core enclosed by an alginate shell in oil-free conditions. The gel allowed permeability of nutrients into the capsule and cell proliferation in a scaffold-free

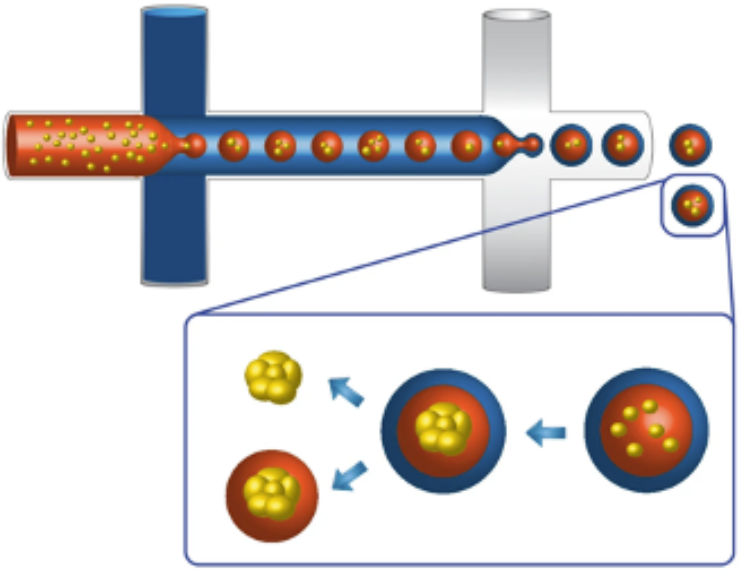
environment, thus integrating mechanical cues from tumor microenvironment. The mean radius of the capsules generated was 100-150 μm and shell thickness varied between 5 and 35 μm.[32]

Furthermore, microencapsulated homotypic or heterotypic hepatocyte spheroids (PMEF, HepG2, and Caco-2 cell types) have also been generated using high-throughput double emulsion droplets in "two polydimethylsiloxane (PDMS) flow-focusing microfluidic devices connected serially" **(Fig. 7A)**.[33] The core diameter of droplets could also be tuned between 65 – 90 μm in the device with channel width 100 μm and from 150 – 200 μm in the device with channel width 200 μm by changing the oil flow rate. Moreover, the spheroid size was dependent on the initial cell density. A concentration of $2x10^6$ cells/mL yielded 8 cells on average in a 200 μm droplet, yielding spheroid size of ~36 μm. Alginate-collagen encapsulation was observed to perform better than alginate encapsulation as evidenced by improved hepatocyte functions during 24-day culture. The encapsulation technique in this study showed high-yield and versatility for liver tissue engineering.[34]

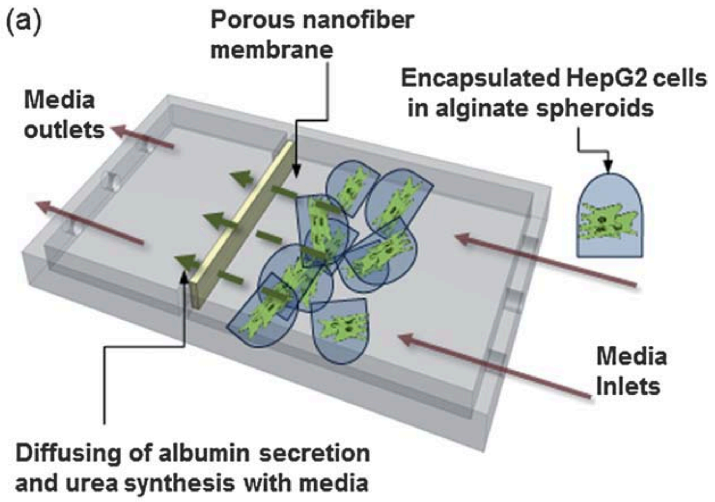
3D bioprinting of cells in a rapid tissue fabrication technique to evaluate normal and pathogenic conditions has also recently come to light as a potential method for constructing complex 3D tissue structures for implantation and regenerative medicine.[35] Adipose-derived stromal vascular fraction cell spheroids were generated by mixing human fat-derived stromal vascular cell fractions in 1.5% (w/v) alginate solution and varying fabrication conditions. They were then placed in spinner culture to access spheroid viability and integrity, which remained viable for 16 days.[35]

In another study, HepG2 cells seeded at an initial density of $4x10^5$ cells/mL and cultured for two days were aggregated in PDMS-based concave molds for spheroid generation,[36] where spheroid diameter could be controlled by the mold size. This method decreased stress on the spheroids because of the lack of transfer steps and most cells showed ~95% viability after encapsulation process **(Fig. 7B)**.

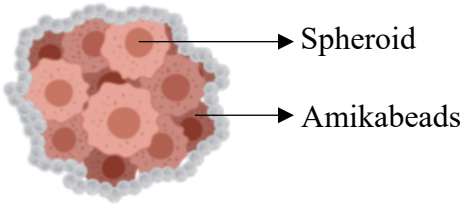
While there are various studies available on encapsulation of spheroids in alginate,[34,36–40] the model is highly complex and cost-intensive in nature. Moreover, the low throughput and size heterogeneity of yield obtained from these techniques inhibit their application in high capacity studies such as drug delivery testing. To overcome these limitations, spheroid encapsulation in aminoglycoside antibiotic-derived microbeads, *Amikabeads*, using a convenient and high throughput method is reported, as illustrated in **Fig. 7C**.



A.



B.



C.

Fig. 7. Encapsulation of spheroids. A. Schematic of how double emulsion (DE) droplets are generated and spheroids are formed. Cells encapsulated in DE droplets assemble to form a single spheroid, which can be subsequently released with or without microgel encapsulation.[6] B. Schematic diagram of the perfusable bio-artificial liver (BAL) chip.[7] C. Process for bioprinting spheroids Amikabeads-encapsulated spheroid. *(Created with BioRender.com)*

[6] Reprinted from Chan, H. F., Zhang, Y. & Leong, K. W. Efficient One-Step Production of Microencapsulated Hepatocyte Spheroids with Enhanced Functions. *Small* **12**, 2720–2730 (2016), permission not required for non-commercial/academic purposes.

[7] Figure and caption reprinted with permission from Lee, K. H. *et al.* Diffusion-mediated in situ alginate encapsulation of cell spheroids using microscale concave well and nanoporous membrane. *Lab Chip* **11**, 1168–1173 (2011).

1.7 Amikabeads – A Hydrogel Microbead Platform

Aminoglycosides and aminoglycoside-derived materials have been used for molecular biology applications – DNA binding and delivery,[41–43] but aminoglycoside antibiotic (amikacin) derived microbeads, *Amikabeads*, have recently come into light as a potential versatile platform for regenerative medicine applications.[44] As discussed before, the existing methods for spheroid encapsulation and investigation of cellular progression or delivery of compounds are low throughput and involve specialized equipment or training. On the other hand, Amikabeads are positively charged microbeads in the diameter range of ~9 ± 4 μm.[44] It is hypothesized that the charge interactions between positively charged Amikabeads and negatively charged components of plasma membrane such as phospholipids, glycolipids, and glycoproteins in cells could play a part in the robust encapsulation of spheroids with Amikabeads without addition of any chemicals or equipment, as illustrated in **Fig. 8**. Amikacin consists of four primary amines and one secondary amine. The amine moieties on Amikabeads can also be quaternized using cationizing agents in aqueous solutions (Amikabeads-Q). This could lead the quaternary amine groups to permanently retain the positive charge at certain pH values[44] and thus, potentially enhance the encapsulation efficiency. Amikabeads also consist of various conjugable groups, which are critical for molecule loading and delivery and can be exploited for regenerative medicine applications.

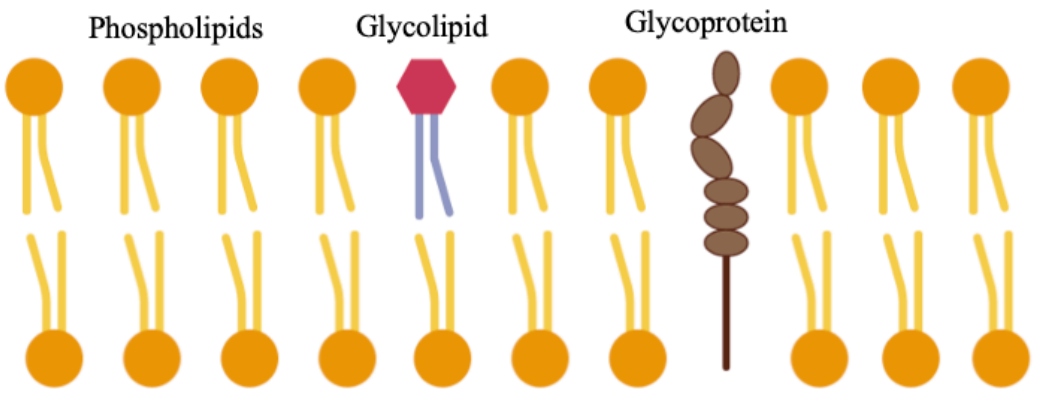


Fig. 8. Plasma membrane of cells. Cell surface consists of negatively charged entities such as phospholipids, glycolipids, and glycoproteins that could interact with the positively charged Amikabeads to generate an encapsulated model held together by charge interactions. (Note: representative figure only, not to scale.) *(Created with BioRender.com)*

1.8 3D Models in Regenerative Medicine and Tissue Engineering

Spheroids exhibit a wide range of intensive intracellular interactions and diffusive mass transport properties that are not seen in 2D culture of cells. Subsequently, their use in tissue engineering is on the rise and various sophisticated techniques have been developed.[45] **Fig. 9** demonstrates the applicability of spheroids in regenerative therapies.

Mesenchymal Stem Cells (MSCs) have long been considered as multifunctional agents for applicability in degenerative disease and immunological disorder treatments.[46–48] Spheroid formation in MSCs have been known to show anti-inflammatory effects and enhanced repair and regenerative properties.[48] Increased angiogenesis and post-transplant survival of MSCs, along with delayed in vitro replicative senescence has also been observed, as illustrated in **Fig. 10**[48]. This has been tested in enhancement of wound regeneration[49,50] and alleviation of side effects for cancer patients after chemotherapy.[51]

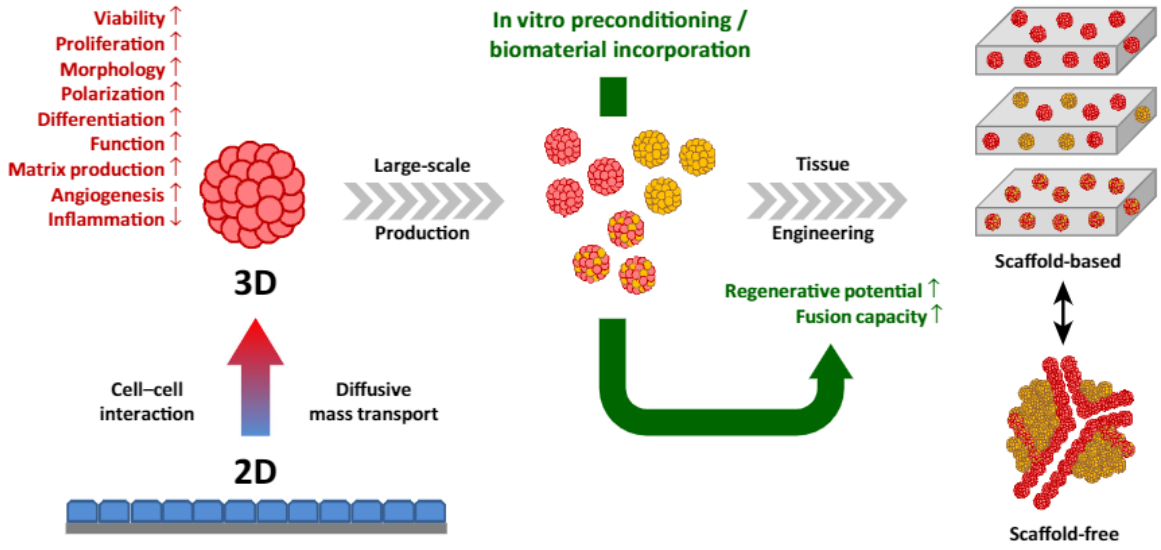


Fig. 9. Application of spheroids in tissue repair and regeneration. As a result of the multidimensional structure of spheroids, they exhibit enhanced repair and regeneration properties such as cell viability, proliferation, differentiation, and angiogenesis. For their generation, monoculture spheroids of different cellular origins are combined or co-cultured. In vitro preconditions play a huge role in the improvement of regenerative potential of spheroids and their fusion capacity.[8]

One of the most promising strategies for regenerative therapy is transplantation. The current transplantation drawbacks such as limited cellular supply and cumbersome cell collection process,[52] lead to issues such as infection, inflammation, and host rejection.[53] On the other hand, injectable spheroids of stem cells have been reported to improve the engraftment efficiency after transplantation.[54–56] Post implantation, MSCs could be induced to differentiate into suitable cells for reconstruction of the defective site.

[8] Figure and caption reprinted from Laschke, M. W. & Menger, M. D. Life is 3D: Boosting Spheroid Function for Tissue Engineering. *Trends Biotechnol* **35**, 133–144, Copyright 2017 with permission from Elsevier.

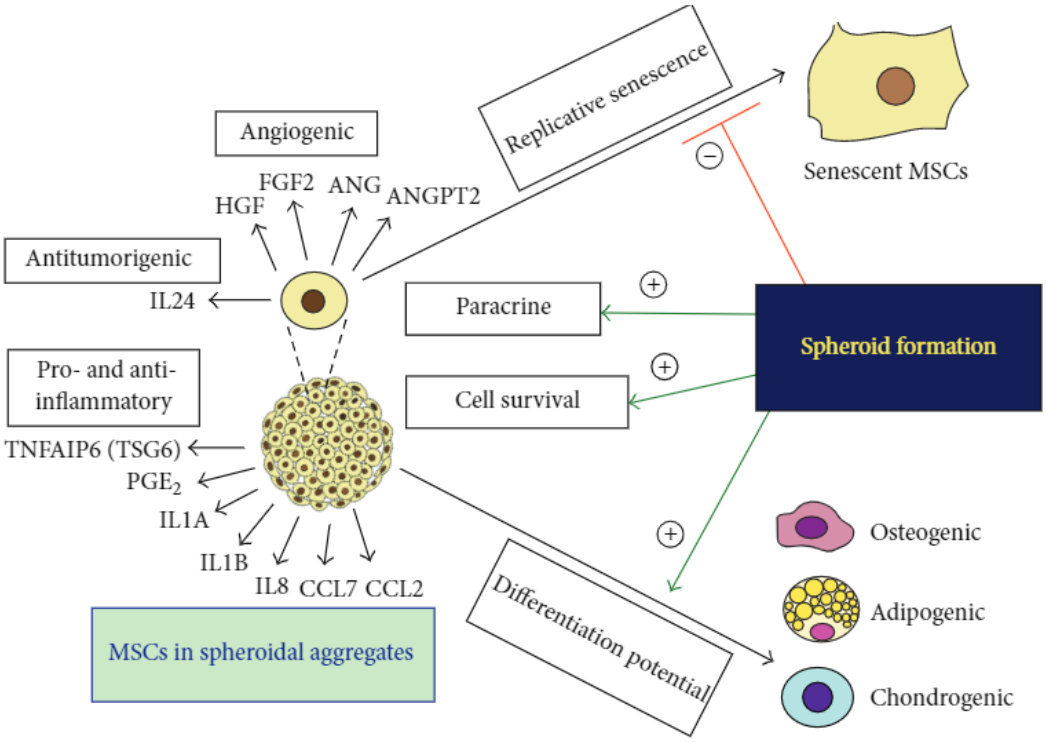


Fig. 10. Clinical significance of MSC spheroids. Spheroidal aggregates are known to (i) enhance paracrine secretion of angiogenic, antitumorigenic, pro- and anti-inflammatory factors, (ii) improve cell survival, (iii) increase differentiation potentials, and (iv) delay replicative senescence of MSCs. (ANG: angiogenin; ANGPT2: angiopoietin 2; CCL2: chemokine (C-C motif) ligand 2; CCL7: chemokine(C-C motif) ligand 7; FGF2: fibroblast growth factor 2; HGF: hepatocyte growth factor; IL1A: interleukin 1α; IL1B: interleukin 1β; IL8:interleukin 8; IL24: interleukin 24; PGE2: prostaglandin E2; TNFAIP6 (TSG6): tumor necrosis factorα-induced protein 6 (tumor necrosis factor α stimulated gene/protein 6); VEGFA: vascular endothelial growth factor-A).[9]

1.9 Overview

Recent advances in regenerative and repair therapies offer areas of improvement and novelty in treatment. This thesis research investigates the use of 3D tumor and stem cell

[9] Figure and caption reproduced from Cesarz, Z. & Tamama, K. Spheroid Culture of Mesenchymal Stem Cells. *Stem Cells Int* **2016**, 1–11 (2016). Copyright © 2016 Zoe Cesarz and Kenichi Tamama. Open access article distributed under the Creative Commons Attribution License.

spheroids generated on Amikagel platform as potential systems for tissue engineering and regenerative therapies, as discussed above. Here, a novel microbead encapsulated 3D spheroid system is reported.

The aim of this research is to develop a hydrogel microbead-encapsulated spheroid platform to study the local delivery of bioactive materials from Amikabeads to cells and engineer multicellular 3D constructs to investigate their implications in potential clinical regenerative medicine applications.

CHAPTER 2

MATERIALS AND METHODS[10]

2.1 Amikagel Synthesis

Amikagel was prepared through ring-opening polymerization between anime groups of Amikacin Hydrate (AH; Sigma Aldrich Inc., St. Louis, MO) and epoxide groups of poly(ethylene glycol)diglycidyl ether (PEGDE; Sigma Aldrich Inc., St. Louis, MO).[31] Monomer AH and cross-linker PEGDE were dissolved in Nanopure® water (NPW) in different stoichiometric ratios to obtain Amikagels of different compositions, named as AM1, AM2, AM3, AM4, AM5, AM6, and AM7 (**Table 4**). All the solutions were vortexed for a minute each until transparency was achieved to ensure complete dissolution.

Table 4. Amikagel compositions used for spheroid generation

Amikagel Compositions		
Amikagel	**Mole Ratio (AH: PEGDE)**	**NPW**
AM1	1: 1.5	100 mL
AM2	1: 2	100 mL
AM3	1: 2.7	100 mL
AM4	1: 3	100 mL
AM5	1: 4	100 mL
AM6	1: 5	100 mL

[10] Studies were performed in collaboration with Mr. Rajeshwar Nitiyanandan, doctoral student in Rege Bioengineering Laboratory.

Amikagel Compositions		
AM7	1: 6	100 mL

2.2 Generation of Amikagel Coated Cell Culture Plates

1 mL AM1-7 pre-gel solutions were filtered through a 0.20 μm filter and 40 μL of filtrate was added to each well of 96 well cell culture plates (polystyrene plates, Corning, NY; glass bottom plates for confocal microscopy, Cellvis, Mountain View, CA). The plates were sealed with Paraffin tape, and incubated in an oven maintained at 40°C for 7.5 h. After gelation, the surface of Amikagel coated wells were washed by adding 275 μL NPW to each well and incubating at 37°C for 12 h to treat traces of untreated monomers. The gel thickness has been reported to be approximately 1 mm on the well surface.[31]

A similar protocol was followed for generation of Amikagel coated 24 well cell culture plates. In each well, 400 μL of filtrate was instead of 40 μL and monomer washing was performed by adding 2750 μL of NPW to each well.

2.3 Cell Culture

T-47D breast cancer and A375 *NRAS*-mutant isogenic melanoma cell lines were obtained from the American Type Cell Culture (Manassas, VA). Normal bone marrow derived Human Mesenchymal Stem Cells (hMSCs) were obtained from Lonza (PT-2501)[11]. Both

[11] Cell line was obtained from Dr. Julianne Holloway's Lab at Arizona State University.

tumor and stem cells were cultured in Dulbecco's Modified Eagle's medium (DMEM) (Sigma, St. Louis, MO) supplemented with 10% v/v Fetal Bovine Serum (FBS), 1% penicillin-streptomycin solution (Corning, Corning, NY) (10,000 units/mL), and 1% 100X GlutaMAX^{TM} solution (gibco, Waltham, MA) at 37°C in 5% carbon dioxide (CO_2) in an incubator. At approximately 80% confluence, cells were trypsinized using 0.25% trypsin-EDTA (Sigma, St. Louis, MO) and sub-cultured.

2.4 Generation of 3D Spheroids

T-47D and A375 cells were seeded at the densities of 30,000 – 100,000 cells/well in 96 well and 750,000 – 1000,000 cells/well in 24 well AM5 coated cell culture plates. hMSCs were seeded at the densities of 30,000 cells/well in 96 well AM1-7 coated cell culture plates to observe robust spheroid formation. The plates were sealed with Paraffin tape and incubated at 37°C in 5% carbon dioxide (CO_2) in an incubator and allowed to form spheroids. Spheroids were formed overnight in case of tumor cells and in 48 hours in case of hMSCs following culture on Amikagel.

2.5 Preparation of Parental Amikabeads[12]

Emulsion polymerization method[57] was used to prepare Amikabeads-P (P: parental) using a technique reported by Grandhi et al.[44] A uniform mixture was generated by dissolving AH (100 mg, 0.17 mmol) in 1 mL of NPW followed by addition of PEGDE in a molar ratio

[12] Prepared by Mr. Subhadeep Dutta, doctoral student in Rege Bioengineering Laboratory.

of 1:2. The mixture was stirred at 100 revolutions per minute (RPM) and pre-gelled for 4 min at 70°C. After 4 min, it was collected in a syringe and dispensed slowly into a solution of mineral oil (Acros Organics, Pittsburgh, PA) and 1% (w/v) Span-80 (TCI America, Portland, OR) through BD Precision Glide 27G1 1/4 needle and 5 mL syringe (Becton, Dickinson and Company, Franklin Lakes, NJ). The mineral oil-surfactant solution was maintained at 65°C throughout the process. Approximately 500 µL of the pre-gel solution was dispensed into the heated oil phase within 25 min under constant stirring at 260 RPM. The beads (Amikabeads-P) could gel for 10 min, followed by extensive washing and size measurements.

Amikabeads-Q were collected by centrifugation for 10 min at 5500 RPM. Oil was washed off their surface by using a solution of ~1% (v/v) Tween 20 detergent. Following detergent washes, the beads were finally washed multiple times with NPW.

2.6 Preparation of Quaternized Amikabeads[13]

Amines and hydroxyls present in Amikabeads-P were quaternized to form Amikabeads-Q (Q: quaternized) using the procedure reported by Grandhi el al.[44] Glycidyl trimethylammonium chloride (GTMAC) was used in an aqueous solution with Amikabeads-P. Excess GTMAC was mixed with Amikabeads at 200 RPM in NPW for 24 h at 70°C followed by extensive washing.[58] The resulting dispersion was termed as Amikabeads-Q.

[13] Prepared by Mr. Subhadeep Dutta, doctoral student in Rege Bioengineering Laboratory.

2.7 Ninhydrin Assay[14]

Quaternization was qualitatively confirmed in Amikabeads-Q dispersion using the ninhydrin assay.[41] Commercially available ninhydrin reagent (200 µL) was added to 1 mg of Amikabeads-P and -Q and incubated at 99°C for 10 min, and the color change was visually observed and recorded.

2.8 Encapsulation of Spheroids

10 mg/mL stock concentrations of Amikabeads-P and Amikabeads-Q were prepared using the methods detailed above. Next, six serial dilutions – 2X, 5X, 10X, 20X, 50X, and 100X were prepared in DMEM. After robust spheroid formation, 100 µL media was slowly removed from the wells containing the spheroids. The spheroids were visualized under the microscope to ensure there was no breakage. 100 µL of each dilution of either Amikabeads-P or Amikabeads-Q was added to the wells. The cell culture plates were then slow centrifuged at 100 RPM for a period of 15 min to accelerate the encapsulation of spheroids with Amikabeads.[15] Post washing three times with 1X PBS to remove stray Amikabeads, the spheroids were imaged with phase-contrast to visualize the encapsulating layer.

[14] Performed in collaboration with Mr. Subhadeep Dutta, doctoral student in Rege Bioengineering Laboratory.
[15] Method developed by Mr. Rajeshwar Nitiyanandan, doctoral student in Rege Bioengineering Laboratory.

2.9 Conjugation of Amikabeads with Rhodamine B[16]

Amikabeads were conjugated with Rhodamine B (Rho-conjugated Amikabeads) containing carboxylic acid groups using COMU ((1-Cyano-2-ethoxy-2oxoethylidenaminooxy) dimethylamino-morpholino-carbenium hexafluorophosphate) catalyzed aqueous-phase reaction. Approximately 40 mg of Amikabeads were dispersed in 5 mL of NPW. In this aqueous solution, 500 µL of 5 wt% TPGS-750-M (DL-α-Tocopherol methoxypolyethylene glycol succinate solution) and 100 µL of 2,6-Lutidine was added to activate the conjugation reaction. Afterwards, 580 µL of 1mM Rhodamine-B was added into the reaction mixture along with 150 mg of COMU, the coupling reagent. Reaction mixture was stirred at room temperature for 12 hours, following which the Rho-conjugated Amikabeads were isolated by centrifuging the solution. They were further washed thrice with NPW to remove unreacted chemicals and further used for encapsulating the spheroids.

2.10 Conjugation of Amikabeads with Fluorescein[17]

Amikabeads were also conjugated with Fluorescein (also containing carboxylic acid groups) using EDC (N-(3-Dimethylaminopropyl)-N′-ethylcarbodiimide hydrochloride) and NHS (N-Hydroxysuccinimide)-catalyzed aqueous-phase reaction. Approximately 40 mg of Amikabeads were dispersed in 5 mL of water. 130 mg of EDC and 80 mg of NHS were added to this aqueous solution and it was stirred for 1 hour at room temperature. 400 µL of 1 mM Fluorescein was added into the reaction mixture and it was stirred at room

[16] Prepared by Mr. Subhadeep Dutta, doctoral student in Rege Bioengineering Laboratory.
[17] Prepared by Mr. Subhadeep Dutta, doctoral student in Rege Bioengineering Laboratory.

temperature for 24 hours. Fluorescein-conjugated beads were isolated by centrifuging the solution and further washed thrice with NPW to remove unreacted chemicals and further used for encapsulating the spheroids.

2.11 Encapsulation of Spheroids in Rho-conjugated Amikabeads

10 mg/mL stock dispersions of Rho-conjugated Amikabeads-P and Amikabeads-Q were prepared using the methods described above. Using these, three working concentrations designated as Low (0.15 mg/mL), Medium (0.75 mg/mL), and High (1.5m g/mL) of both Amikabeads-P and Amikabeads-Q were prepared in DMEM and tested for encapsulation (**Table 5)**.

Table 5. Rho-conjugated Amikabeads-P and -Q working dispersions used for spheroid encapsulation

Rho-conjugated Amikabeads	
Stock Concentration	**Working Concentrations**
Amikabeads-P (10 mg/mL)	Low (0.15 mg/mL)
	Medium (0.75 mg/mL)
	High (1.5 mg/mL)
Amikabeads-Q (10 mg/mL)	Low (0.15 mg/mL)
	Medium (0.75 mg/mL)
	High (1.5 mg/mL)

As described above, the spheroids were encapsulated in the above-mentioned working concentrations of Rho-conjugated Amikabeads. Before centrifugation, the corresponding volume of fluorescent label for staining the spheroid as mentioned above was also added for contrast. The resulting encapsulated spheroids were termed as Rho-conjugated Amikabeads encapsulated spheroids.

2.12 Encapsulation of Spheroids in Fluorescein-conjugated Amikabeads

10mg/ml stock dispersions of Fluorescein-conjugated Amikabeads-P and Amikabeads-Q were prepared using the methods described above. Using these, six working concentrations of both Amikabeads-P and Amikabeads-Q prepared in DMEM were tested for encapsulation (**Table 6)**.

As described above, the spheroids were fluorescent labeled and encapsulated in the above-mentioned working concentrations of Fluorescein-conjugated Amikabeads. The resulting encapsulated spheroids were termed as Fluorescein-conjugated Amikabeads encapsulated spheroids.

Table 6. Fluorescein-conjugated Amikabeads-P and -Q working dispersions used for spheroid encapsulation

Fluorescein-conjugated Amikabeads	
Stock Concentration	**Working Concentrations**
Amikabeads-P (10 mg/mL)	2X (5 mg/mL)
	5X (2 mg/mL)
	10X (1 mg/mL)
	20X (0.5 mg/mL)
	50X (0.2 mg/mL)
	100X (0.1 mg/mL)
Amikabeads-Q (10 mg/mL)	2X (5 mg/mL)
	5X (2 mg/mL)
	10X (1 mg/mL)
	20X (0.5 mg/mL)
	50X (0.2 mg/mL)
	100X (0.1 mg/mL)

2.13 Fluorescence Intensity Optimization

The concentration of Fluorescein-conjugated Amikabeads used for encapsulation was optimized by preparing serial dilutions (as mentioned in **Table 6**) of Amikabead stock dispersion in DMEM. The fluorescence intensity of serial dilutions was measured using a fluorometric plate reader and plotted against the concentrations.

All concentrations were then used to encapsulate the spheroids and observed through confocal microscopy, as mentioned above, to visually choose the optimum intensity. The corresponding concentration of Fluorescein-conjugated Amikabead dispersion was used for further encapsulation studies.

2.14 Fluorescence Labeling of Spheroids

Five fluorescent dyes were used to label spheroids to provide contrast for confocal microscopy as detailed in **Table 7**.

The corresponding volume of fluorescent dyes was added along with the Amikabeads dispersion before centrifugation to allow optimal spheroid labeling, as mentioned in the sections above.

Table 7. Fluorescent labels used to stain spheroids

Spheroid Stains				
Stain	**Role**	**Working Concentration, Volume Used**	**Maximum $\lambda_{absorption}$**	**Maximum $\lambda_{emission}$**
4′,6-diamidino-2-phenylindole (DAPI)	Fluorescent stain binding to the adenine-thymine-rich regions of DNA	1 µg/mL prepared in 1X PBS, 5 µl/well	358 nm	461 nm
Hoechst 33342 (Thermo Scientific™, Waltham, MA)	Cell permeant nuclear counterstain emitting blue fluorescence	1 mg/mL in 1X PBS, 0.5 µl/well	352 nm	454 nm
DRAQ5™ (AAT Bioquest, Inc.,Sunnyvale, CA)	A far-red emitting anthraquinone compound staining nuclei in live cells	10 µM prepared in 1X PBS, 50 µl/well	598/646 nm	681/697 nm
CytoTrace™ Red CMTPX (AAT Bioquest, Inc., Sunnyvale, CA)	A fluorescent cell-permeable dye for tracing cells	2 µM prepared in DMSO, 0.5 µl/well	577 nm	602 nm
Concanavalin A (Con A) CF Dye (Biotium, Inc., Fremont, CA)	A cell surface stain for mammalian cells	50 µg/mL prepared in sterile NPW	593 nm	614 nm

2.15 Phase Contrast Microscopy

The encapsulated spheroids were visualized under EVOS FL Auto Live Cell Imaging Inverted Microscope System (Advanced Light Microscopy Core – Regenerative Medicine and Bioimaging Facility, Arizona State University Core Facilities) to capture phase contrast images. 96 well polystyrene cell culture plates containing encapsulated spheroids were observed using 4X objective lens.

2.16 Laser Scanning Confocal Microscopy

The encapsulated spheroids used for confocal microscopy were generated on glass-bottom 96 well cell culture plates and imaged under Leica TCS SP8 White Light Laser Scanning Confocal with Light Sheet Microscope (Advanced Light Microscopy Core – Regenerative Medicine and Bioimaging Facility, Arizona State University Core Facilities). The microscope is equipped with white light tunable laser as well as an Argon 488 nm and 405 nm lasers. The system also has a combination of PMT and HyD GaAsP detectors as well as a DIC bright field detector. The fluorescent labels on Amikabeads and spheroids provided the contrast, and the images were captured using a 10X objective lens and a compilation of 30-40 sections of 5 μM each were used to reconstruct the 3D z-stack of the encapsulated spheroid.

2.17 Confocal Microscopy with Dipping Lens[18]

The encapsulated spheroids were washed thrice with 1X PBS to remove stray Amikabeads and fixed using 10% neutral buffered formalin (NBF) overnight. The pointy end of 200 µL autopipette tip was chopped and used to remove encapsulated spheroids from the wells. They were suspended in 60 mm polystyrene petri dishes (Fisher Scientific, Hampton, NH) containing 1X PBS. The suspended spheroids were imaged using the Leica SP5 AcoustoOptical Beam Splitter Spectral Confocal Microscope (Advanced Light Microscopy Core – Regenerative Medicine and Bioimaging Facility, Arizona State University Core Facilities). A 10X high numerical aperture dipping objective with an access angle of 41° and a free working distance of 2.5 mm was employed to capture images.

2.18 Cell Viability Assay

CellTiter-Glo ® 3D Cell Viability Assay was conducted to determine the viable cell population in encapsulated spheroids based on the amount of the ATP present at four different time points (24, 48, 72, 96 h). according to the manufacturer's protocols, 150 µL assay reagent per 96 well glass-bottom cell culture plate (equal to the existing well volume) containing encapsulated spheroids was added and the plate was incubated. It was then manually shaken vigorously for 5 minutes to induce cell lysis and effectively extract ATP from the encapsulated spheroids.

[18] Performed under the guidance of Ms. Page Baluch, Research Scientist, W. M. Keck Bioimaging Laboratory in the School of Life Sciences, ASU.

After allowing incubation at RT for 25 min to stabilize the signal, the luminescence was tested using a plate reader using an integration time of .25 – 1 sec per well. Wells containing only spheroids and only Amikabeads were used as controls to ascertain absence of any background luminescence.

2.19 Flow Cytometry[19]

Flow cytometry preparation involved transferring and dissociating three identical encapsulated spheroids into a single vial and centrifugation at 1000 RPM at 25°C for 10 min. Majority of the supernatant was removed (~90%) and the cell pellet was resuspended in either 200 mL of 1X PBS for control conditions or a mixture of 1X PBS:Triton X:Propidium Iodide at a ratio of 10:1:1 (v/v/v) for treatment conditions. The tubes were placed on ice or a cold rack that had been pre-frozen to -20°C until flow cytometry data was collected. Flow cytometry was run on BD FACSAria Ilu Cell Sorter housed in the Flow Cytometry Facility (Arizona State University Core Facilities).

[19] Performed by Dr. Sara Bowen, Dignity Health at Flow Cytometry Facility, Biodesign Institute, ASU.

CHAPTER 3

RESULTS AND DISCUSSION

3.1 Amikagel Coated Cell Culture Plates

The reaction of amines present in amikacin with epoxides present in PEGDE resulted in the formation of Amikagel as depicted in **Fig. 11**. As summarized in **Table 11**, AM2-7 showed uniform layering on polystyrene cell culture plates, but AM1 coated plates illustrated lumps of gel, advocating the importance of PEGDE (cross-linker). They were henceforth not used for spheroid generation. Possibly due to the change in hydrophobicity, some cracks were observed sparsely among the wells of the glass-bottom plates coated with AM2-7, but majority of them were uniformly coated.

3.2 Formation of Spheroids

Appropriate concentrations of freshly sub-cultured cells were seeded on Amikagel coated plates and incubated for 1-3 days (**Fig. 12A**). T-47D breast cancer and A375 *NRAS*-mutant isogenic melanoma cells demonstrated compact spheroid formation on the surface of AM5, whereas spheroids generated on AM6 and AM7 showed fragility. On the other hand, human bone marrow derived MSCs appeared to demonstrate no adhesivity on AM6 and AM7; loosely spread cells on AM2-AM4 and a cluster of cells prone to breakage was indicated on AM5, as mentioned in **Table 8** and illustrated in **Fig. 12B**. Non-adhesivity on AM5, AM6, and AM7 coated plates was simultaneously brought about by lower amine contents of AH and higher PEG contents caused by the ring-opening polymerization reaction.[30]

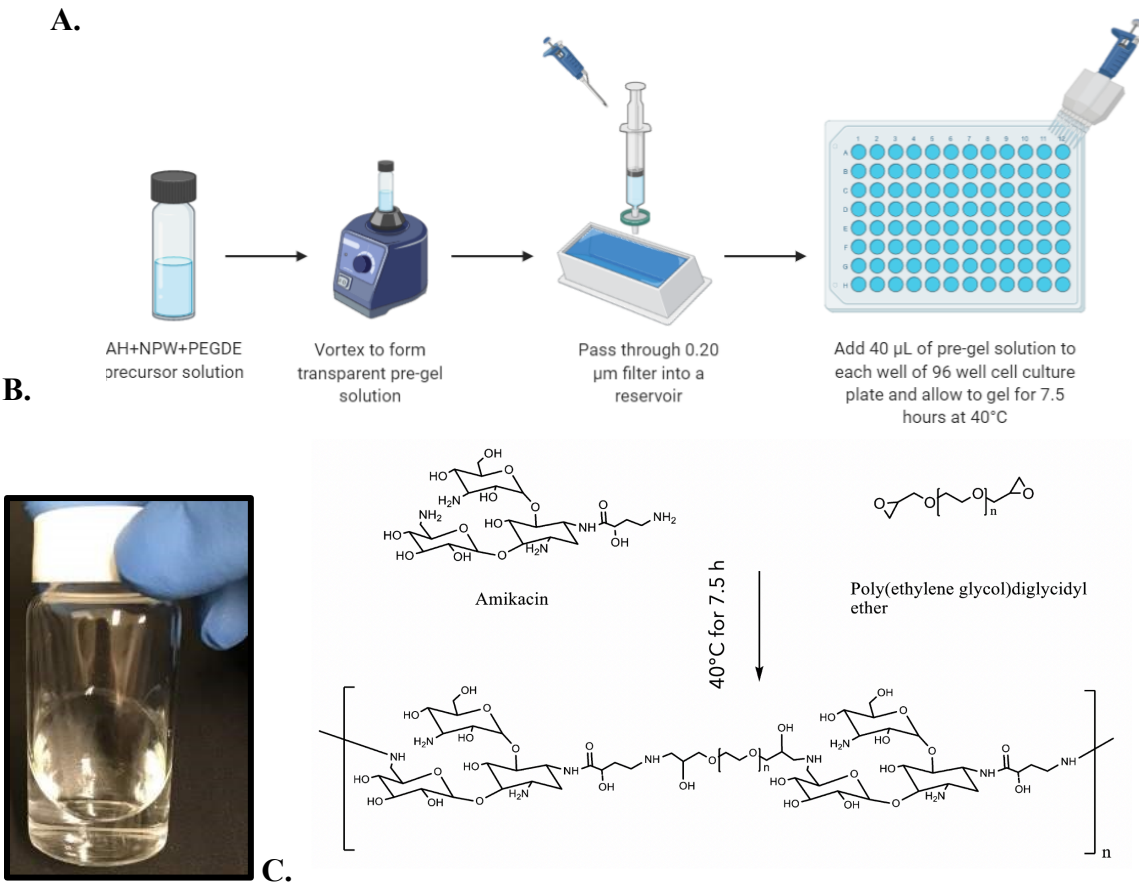


Fig. 11. **Amikagel formation.** A. Schematic of Amikagel formation. *(Created with BioRender.com)* B. Amikacin Hydrate (AH) and Poly(ethylene glycol) diglycidyl Ether (PEGDE) pre-gel solution in NPW before addition to cell culture plates C. Schematic of the reaction between AH and PEGDE, resulting in the formation of Amikagel.[20]

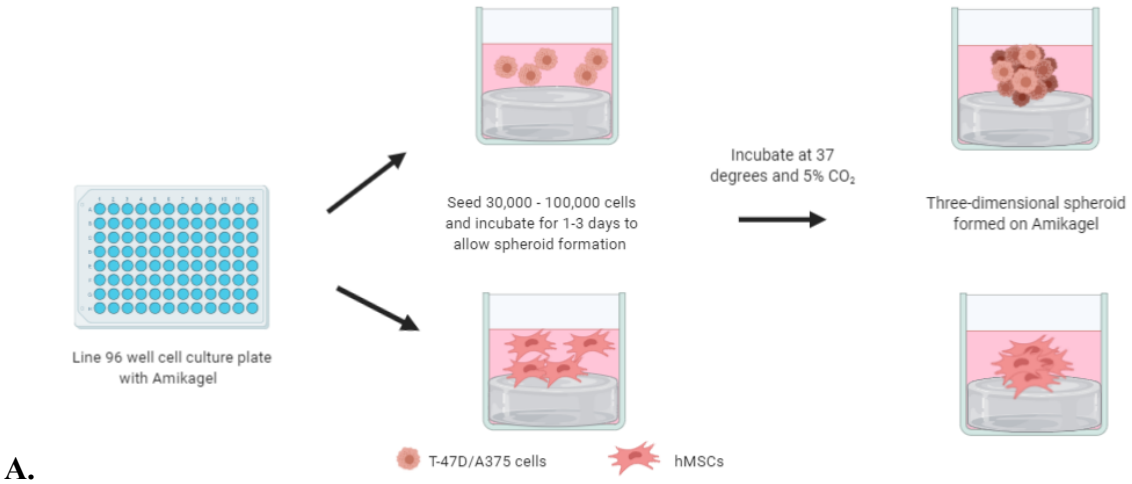
Formation of a single spheroid was observed in every well, likely facilitated by the high reported mechanical stiffness and non-adhesivity of the Amikagel.[30] The size of spheroids was modulating by seeding different cell numbers on Amikagel (30,000/ 50,000/ 750,000/ 100,000 cells/well); the dimensions of spheroids – as approximated from confocal microscopy – could be tuned from ~300 µm to ~1200 µm by increasing cell density. Due

[20] Reprinted (adapted) with permission from Grandhi, T. S. P. et al. Aminoglycoside Antibiotic-Derived Anion-Exchange Microbeads for Plasmid DNA Binding and in Situ DNA Capture. *ACS Appl Mater Inter* **6**, 18577–18589 (2014). Copyright 2014. American Chemical Society.

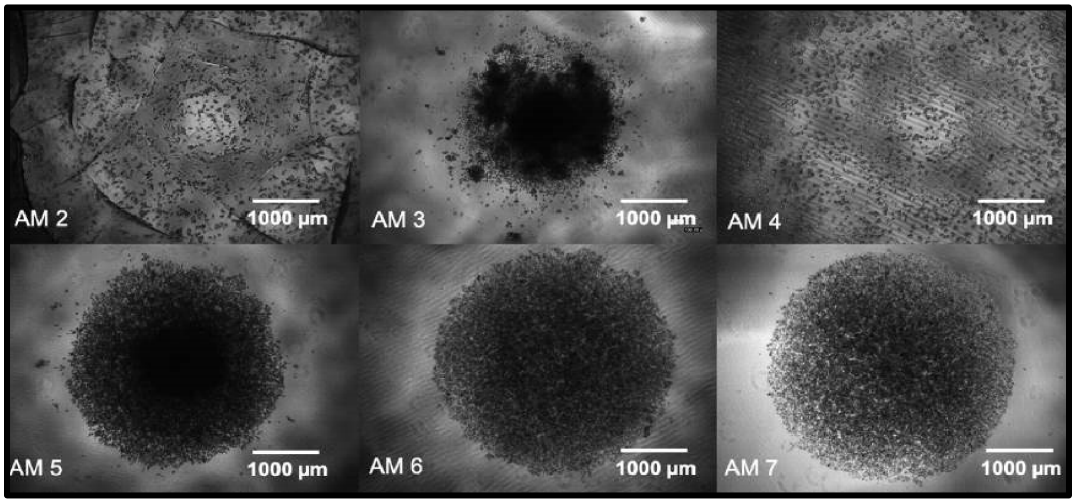
to such ease of use of Amikagel platform, it could potentially facilitate more convenient spheroid formation than other approaches of 3D cell culture involving rotating wall bioreactors[59] and hanging droplet cultures that are labor intensive and provide low throughput and a heterogenous population of spheroids.[60]

Table 8. Spheroid formation on Amikagel coated cell culture plates

Spheroid Formation				
Amikagel	**Uniform Amikagel Coating**		**Spheroid Formation**	
	Polystyrene Plates	**Glass Bottom Plates**	**T-47D and A375**	**hMSCs**
AM1	No	No	No	No
AM2	Yes	Sparse cracks	No	No
AM3	Yes	Sparse cracks	No	No
AM4	Yes	Sparse cracks	No	No
AM5	Yes	Yes	Yes	No
AM6	Yes	Yes	No	Yes
AM7	Yes	Yes	No	Yes



A.



B.

Fig. 12. Spheroid generation. A. Schematic of spheroid generation using Amikagel-coated cell culture plates. *(Created with BioRender.com)* B. Phase-contrast images of hMSC spheroids in 96 well AM2-AM7 coated cell culture plates after 3 days of incubation generated at an initial cell density of 30,000 cells/well. AM2-Am4 evidenced loosely spread cells and a cluster of cells was observed in AM5 which broke down when encapsulation studies were performed. AM6 and AM7 facilitated the formation of homogeneously packed spheroids. Objective: 4X, Scale = 1000 µm. *(Images acquired in collaboration with Mr. Rajeshwar Nitiyanandan, doctoral student in Rege Bioengineering Laboratory)*

3.3 Amikabeads Synthesis[21]

Here, the generation of amikacin derived microbeads, *Amikabeads*, for potential application in encapsulation of spheroids is illustrated. The cross-linking of amines present in AH and epoxides in PEGDE resulted in the formation of Amikagel. It has been reported Amikagel has multiple amine moieties that can be exploited for molecular biotechnology applications.[44] For potential encapsulation of spheroids, Amikabeads-P were generated through emulsion polymerization with AH:PEGDE as 1:2. Based on reported literature,[44] the mixture was allowed to pre-gel for 4 min while stirring at 100 RPM at 70°C. After introducing to mineral oil phase and supplementing with 80% Span-80 surfactant, Amikabeads-P were separated by centrifugation at 5000 RPM for 10 min. The microbeads were then extensively washed with NPW supplemented with 1% (v/v) Tween 20 (**Fig. 13**).

3.4 Amikabeads Characterization

Based on phase contrast images and previous reports, it has been observed that Amikabeads generated using the above emulsion system had spherical morphologies (**Fig 14**) and average diameter varying from ~9 ± 4 μm.[44]

[21] Performed by Mr. Subhadeep Dutta, doctoral student in Rege Bioengineering Laboratory.

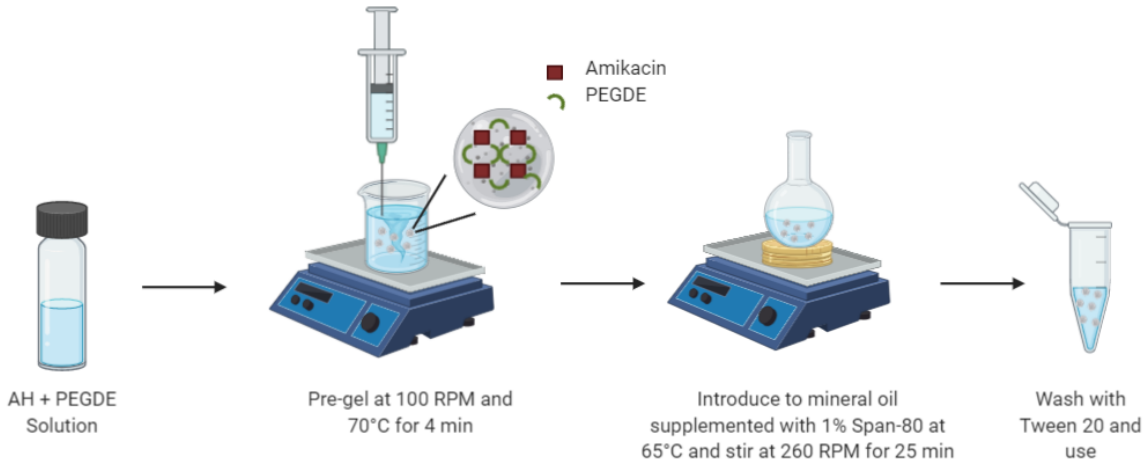


Fig. 13. Synthesis of Amikabeads. *(Created with BioRender.com)*

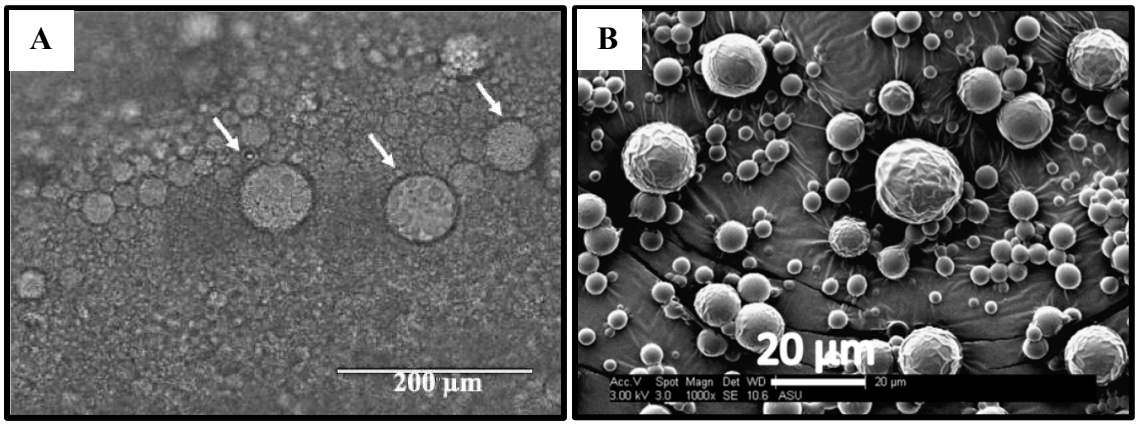


Fig. 14. **Characterization of Amikabeads.** A. Phase contrast image of Amikabeads-P generated using the emulsion polymerization reaction; white arrows denote individual beads with spherical morphology. Scale = 200 µm. B. Scanning electron microscopy (SEM) image of Amikabeads indicates spherical particles with an average diameter of ~9 ± 4 µm, as reported by Grandhi et al. The Amikabeads used for present research likely have similar diameters, but some Amikabeads of diameter ~70-100 µm were also seen. Scale = 20 µm.[22]

[22] Reprinted (adapted) with permission from Grandhi, T. S. P. et al. Aminoglycoside Antibiotic-Derived Anion-Exchange Microbeads for Plasmid DNA Binding and in Situ DNA Capture. *ACS Appl Mater Inter* **6**, 18577–18589 (2014). Copyright 2014. American Chemical Society.

3.5 Quaternization of Amikabeads[23]

To use Amikabeads in loading of bioactive compounds for delivery to spheroids, it is critical that accessible amine moieties which allow for subsequent conjugation chemistries be present. The reaction of 100 µL ninhydrin reagent with a 0.5 mm Amikabead-P model at 70°C for 10 min resulted in the generation of Ruhemann's purple product, which is an evidence of the presence of reactive primary and secondary amines.

Quaternization of these reactive amines during generation of Amikabeads-Q was confirmed by the lack of demonstration of a bluish-purple product, unlike the unmodified Amikabeads-P (**Fig. 15**).

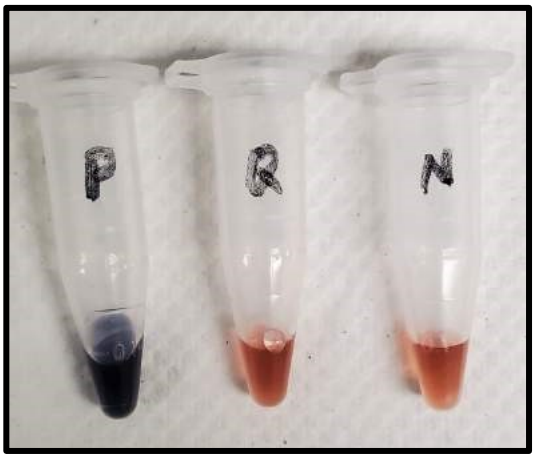
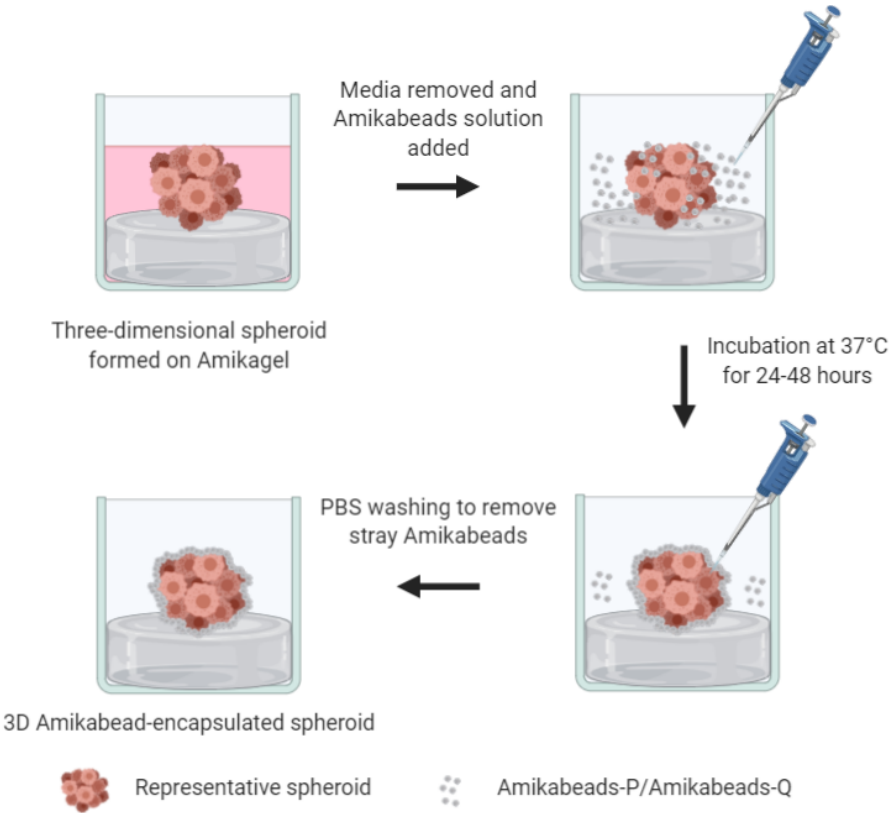


Fig. 15. Ninhydrin assay. Ninhydrin assay illustrating the presence of reactive primary and secondary amines in Amikabeads-P through a bluish-purple product (sample tagged as "P") and the lack of their presence in Amikabeads-Q (sample tagged as "Q") as compared to negative control (sample tagged as "N"). *(Study performed in collaboration with Mr. Rajeshwar Nitiyanandan, doctoral student in Rege Bioengineering Laboratory)*

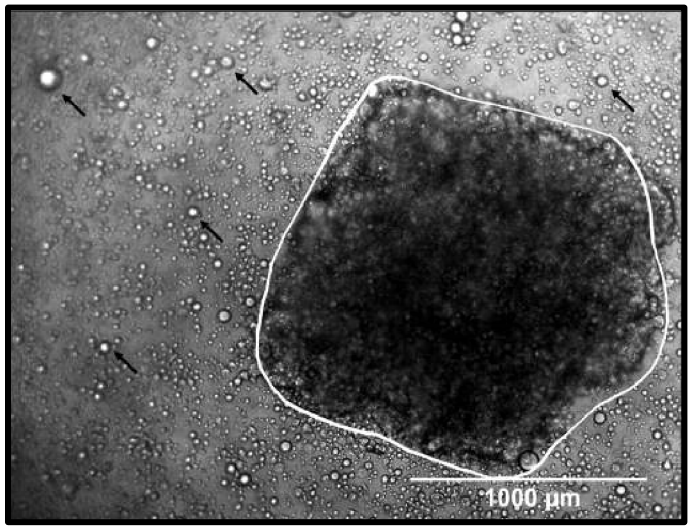
[23] Performed by Mr. Subhadeep Dutta, doctoral student in Rege Bioengineering Laboratory.

3.6 Amikabead-Encapsulated Spheroids

Due to the close proximity and physical confinement of cells in Amikabeads, the Amikabead-encapsulated spheroid model could be substantially beneficial in regenerative medicine, including investigation of delivery of Amikabeads-loaded bioactive compounds and drugs as compared to soluble drug delivery testing. Thus, efforts were focused on ensuring a complete encapsulation of the top- and bottom surfaces, along with the edges of the spheroid with the Amikabeads. Initially, it was hypothesized that the spheroid encapsulation could take place through charge interactions between positively charged Amikabeads and negatively charged phospholipid bilayer of cells if the Amikagel coated plates were allowed to incubate for a long duration of time at 37°C (**Fig. 16A**). Corresponding volumes of the Amikabead-P dilutions were added to wells containing the spheroids and phase contrast images were captured at different intervals under EVOS FL Auto Live Cell Imaging Inverted Microscope System, as described previously (**Fig. 16B**). The images demonstrated that using this technique, encapsulation could only be observed after a period of 48 h. It was also noticed that the encapsulated regions were directly proportional to the concentration of Amikabeads dispersion.



A.



B.

Fig. 16. Addition of Amikabeads for encapsulation. A. Schematic of encapsulation of spheroids in Amikabeads. *(Created with BioRender.com)* B. Representative phase-contrast image of a well containing a T-47D spheroid (in white boundary, in white boundary, initial cell density = 30,000 cells/well) and 100 µL of 0.75 mg/mL Amikabeads-P dispersion (marked by black arrows) at t = 0 (just after addition) in a 96 well cell culture plate using a 4X objective. Scale = 1000 µm. *(Image acquired in collaboration with Mr. Rajeshwar Nitiyanandan, doctoral student in Rege Bioengineering Laboratory)*

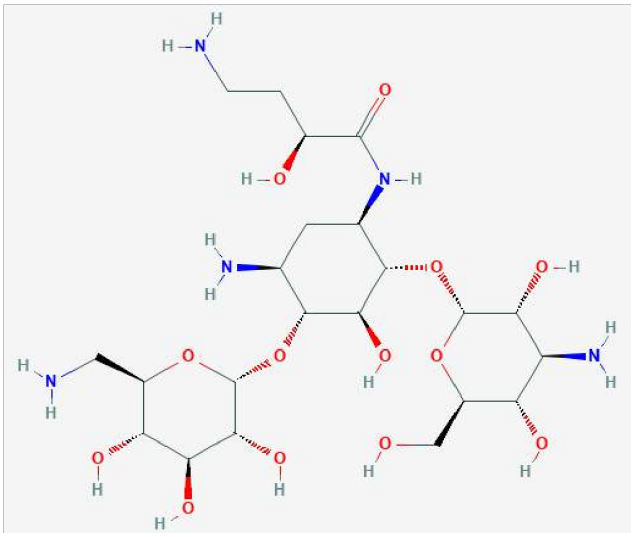


Fig. 17. Amikacin. 2D chemical structure of Amikacin ($C_{22}H_{43}N_5O_{13}$),[8] a broad-spectrum semisynthetic aminoglycoside antibiotic.[61]

Amikacin has four primary amines, one secondary amine, and eight hydroxyl groups (**Fig. 17**).[61] As reported before, quaternization of amine groups can help increase the positive charge content in Amikabeads-Q.[44] The quaternization was performed using GTMAC; the amines of amikacin react with the epoxide group of GTMAC at neutral or acidic pH as an addition reaction.[58] As a result of this, a more efficient spheroid encapsulation was anticipated.

As expected, Amikabeads-Q formed a ring like layer around the T-47D spheroids within 24 hours of incubation and the size and density of the outer ring expanded with an increase in Amikabeads-Q concentration. The encapsulated spheroids were also captured in phase-contrast at a higher resolution to visualize the regions between spheroids and Amikabeads (**Fig. 18**).

[8] 2D structure image of CID 37768 (amikacin) reproduced from National Center for Biotechnology Information (2020). PubChem Compound Summary for CID 37768, Amikacin. Retrieved October 15, 2020 from https://pubchem.ncbi.nlm.nih.gov/compound/Amikacin. (No special permissions required).

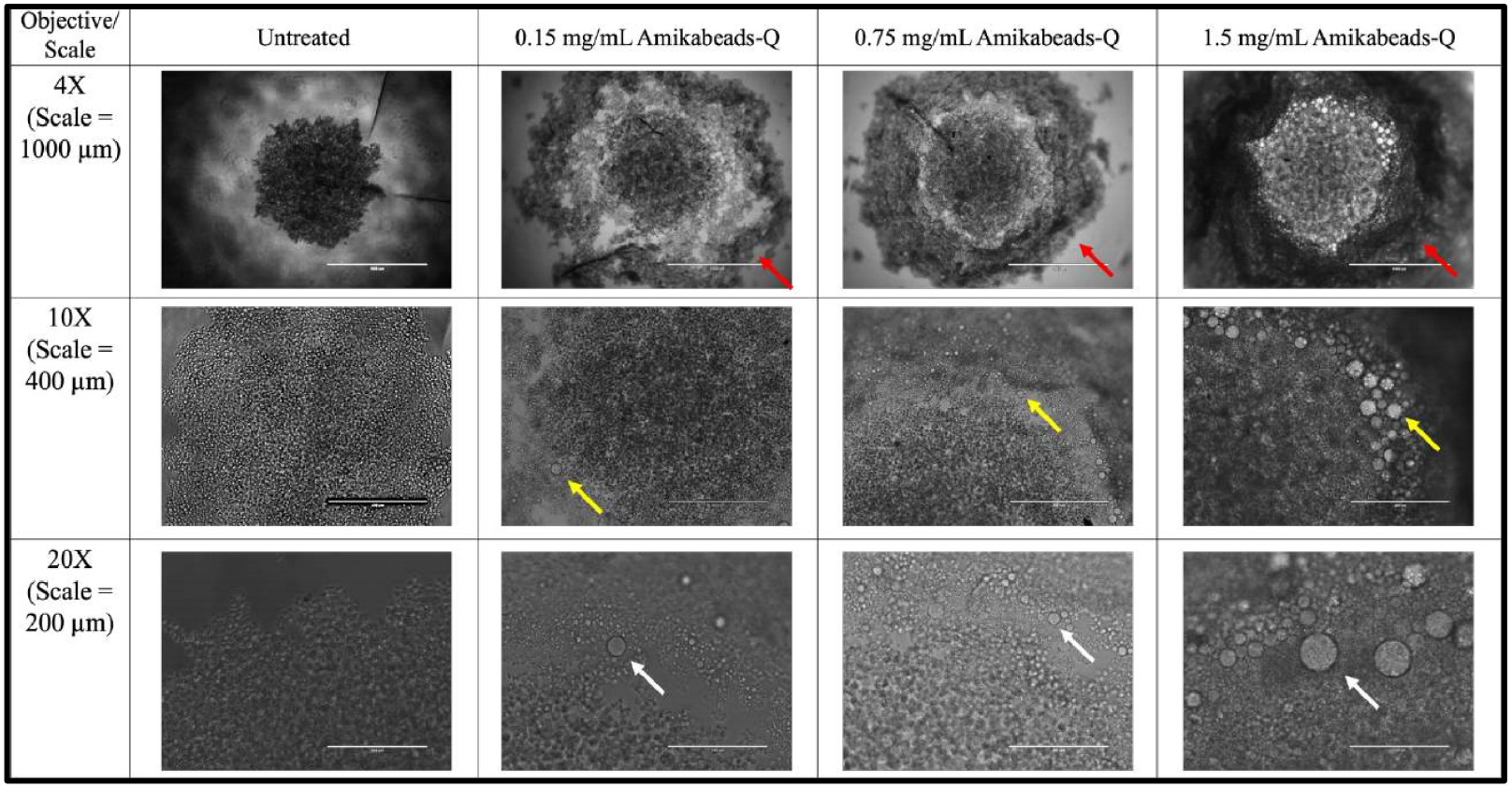
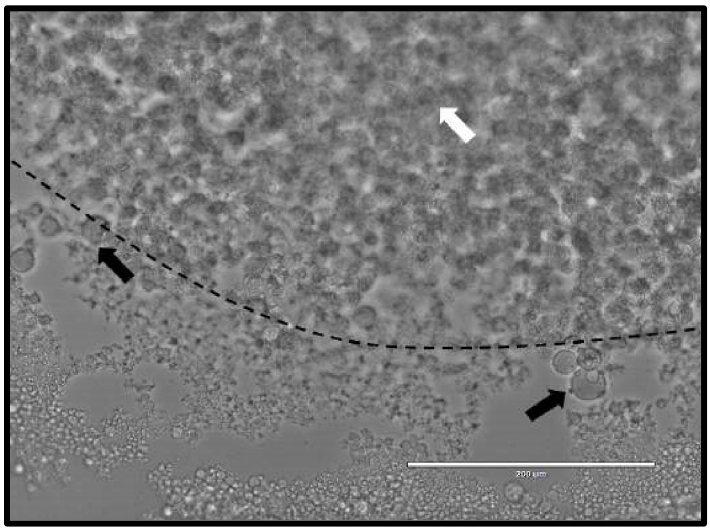


Fig. 18. **Amikabeads-encapsulated T-47D spheroids.** Formation of encapsulation layer around T-47D spheroids (initial cell density = 30,000 cells/well) 24 hours after their incubation with 0.15 mg/ml, 0.75 mg/ml), and 1.5 mg/ml dilutions of Amikabeads-Q as compared to untreated spheroids. Red arrows depict the direct correlation between concentration of Amikabead dispersion and size and density of the encapsulated layer. Yellow and red arrows depict Amikabeads in the encapsulating layer using 10X and 20X objective, respectively. *(Images acquired in collaboration with Mr. Rajeshwar Nitiyanandan, doctoral student in Rege Bioengineering Laboratory)*

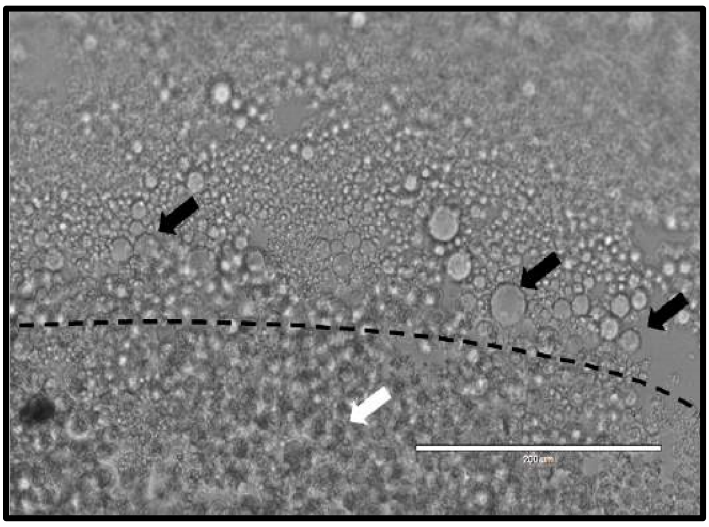
The images strengthened the position that Amikabeads-Q could provide an enhanced encapsulation efficacy as compared to Amikabeads-P with a potential application in delivery of bioactive compounds to the spheroids. Based on this evidence, Amikabeads-Q were used for rest of the studies (henceforth, *Amikabeads*).

Bright field images of encapsulated spheroids using 20X objective proffered a definite region of separation between spheroids and Amikabeads – *the interspersed region* – as shown in **Fig. 19**. This approach, although successful, was of labor and time intensive nature. Multiple artificial means have been utilized to accelerate the encapsulation of spheroids, such as microfluidic devices,[32] emulsion droplets,[33,35] 3D printing,[35] alginate or hydrogel biomaterials,[62,63] but they come with roadblocks such as disintegration of spheroid and low encapsulated cell viability.[64]

A.



B.



C.

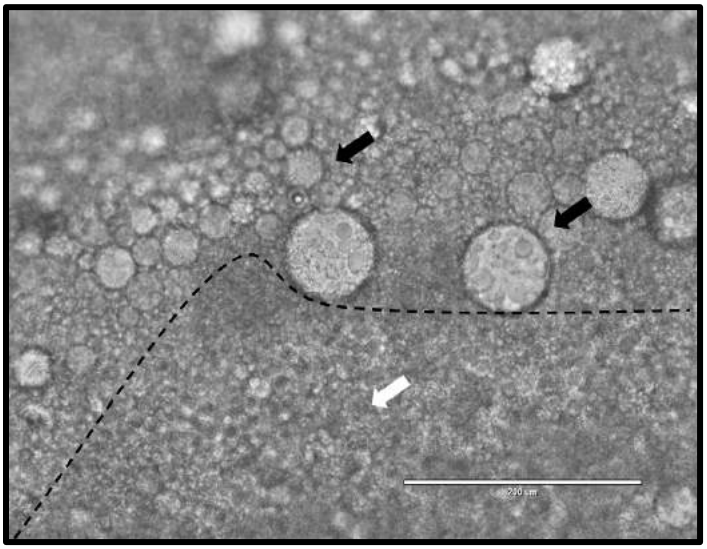
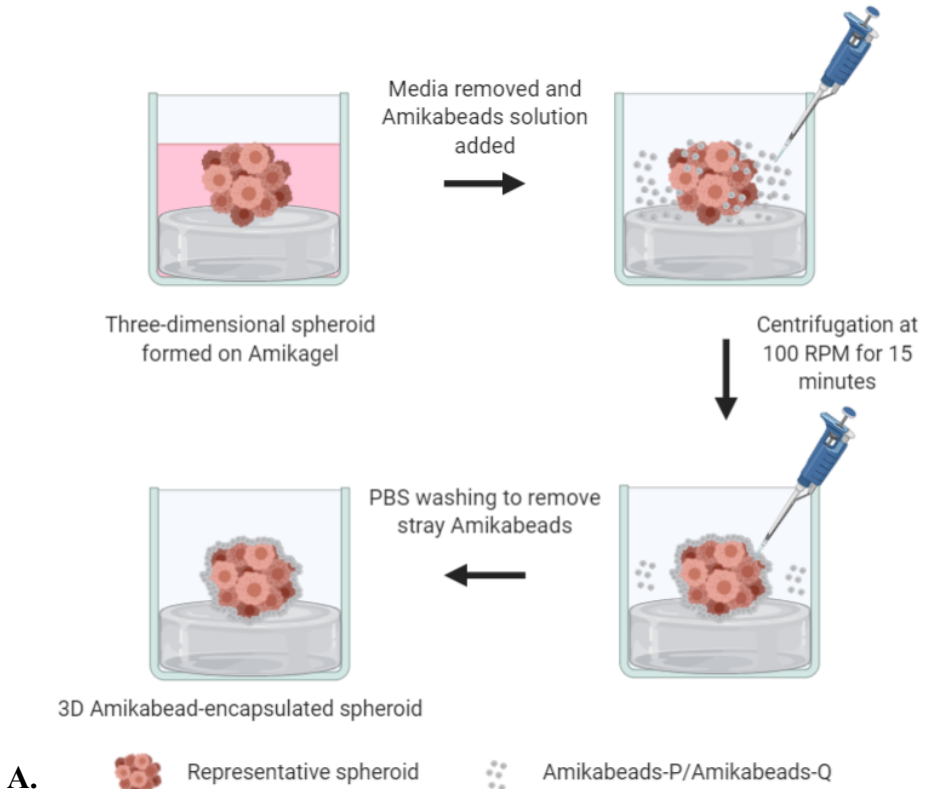


Fig. 19. **Interspersed region between spheroid and Amikabeads.** Bright field microscopy images showing the interspersed region of T-47D spheroids (initial cell density = 30,000 cells/well) with A. 0.15 mg/mL, B. 0.75 mg/mL, and C. 1.5 mg/mL dilutions of Amikabeads-Q solution marked by a black dotted boundary. White arrows indicate the region of spheroids and black arrows indicate the region of the encapsulation layer of Amikabeads-Q. Objective: 20X, Scale = 200 μm. *(Images acquired in collaboration with Mr. Rajeshwar Nitiyanandan, doctoral student in Rege Bioengineering Laboratory)*

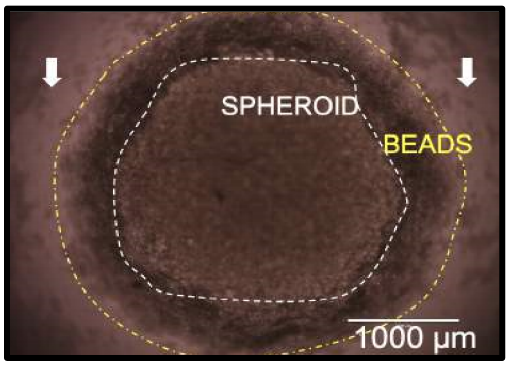
3.7 Low Speed Centrifugation Enhances Encapsulation[24]

Owing to the challenges posed by the previously mentioned and existing encapsulation techniques, low speed centrifugation of cell culture plates containing spheroids after addition of Amikabeads was tested for encapsulation efficiency (**Fig. 20A**). Centrifugation at lower RPMs (100-1000 RPM) for a longer duration of time has been successfully employed to enhance the transfection rate in suspension cell cultures.[65–67] After several trial runs, the optimum RPM and centrifugation time that could lead to adequate encapsulation were identified. The integrity of spheroids was confirmed using bright field microscopy. Centrifuging the plate at 100 RPM for 15 minutes after addition of Amikabeads demonstrated optimum encapsulation, as illustrated in **Fig. 20B-C**.



[24] Method developed by Mr. Rajeshwar Nitiyanandan, doctoral student in Rege Bioengineering Laboratory.

B.



C.

Treatment	Bright field at 4X (Scale = 1000 µm)	Phase-contrast at 4X (Scale = 1000 µm)
0.15 mg/mL Amikabeads-Q		
0.75 mg/mL Amikabeads-Q		
1.5 mg/mL Amikabeads-Q		

Fig. 20. **Spheroid encapsulation using centrifugation.** A. Schematic of encapsulation of spheroids in Amikabeads using low speed centrifugation technique. *(Created with BioRender.com)* B. Representative bright field image demonstrating an Amikabead-encapsulated T-47D spheroid outlined in white (initial cell density = 30,000 cells/well, Amikabead concentration = 1.5 mg/mL). The encapsulated layer boundary is outlined in yellow and free space outside the spheroid is represented by white arrows. C. Bright field and phase-contrast images of T-47D spheroids encapsulated in Amikabeads concentration of 0.15 mg/mL, 0.75 mg/mL, and 1.5 mg/mL. Objective: 4X, Scale = 1000 µm. *(Images acquired in collaboration with Mr. Rajeshwar Nitiyanandan, doctoral student in Rege Bioengineering Laboratory)*

3.8 Fluorescent-Tag Labeled Amikabeads

Rhodamine-B-conjugated Amikabeads: After achieving optimum encapsulation, Amikabeads were conjugated with Rhodamine-B (*Rho-conjugated Amikabeads)*, a red fluorescing tracer dye to visualize the encapsulation through fluorescence and confocal microscopy, as demonstrated in **Fig. 21**. Spheroids were generated using different initial cell densities and encapsulated with Rho-conjugated Amikabeads, as discussed previously.

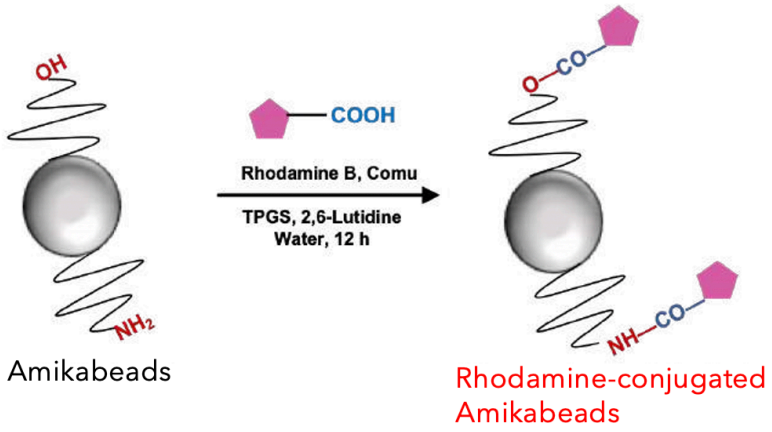


Fig. 21. Rho-conjugated Amikabeads. Schematic of the conjugation of Amikabeads with Rhodamine-B using COMU. (*Rho-conjugated Amikabeads were procured from Mr. Subhadeep Dutta, doctoral student, Rege Bioengineering Laboratory; figure credits: Mr. Subhadeep Dutta)*

Fluorescein-conjugated Amikabeads: To avoid the overlap of red fluorescing signal from Rho-conjugated Amikabeads and red spheroid stains (such as DRAQ5™), Amikabeads were also conjugated with Fluorescein, an organic green fluorescing tracer dye for contrast (**Fig. 22**).

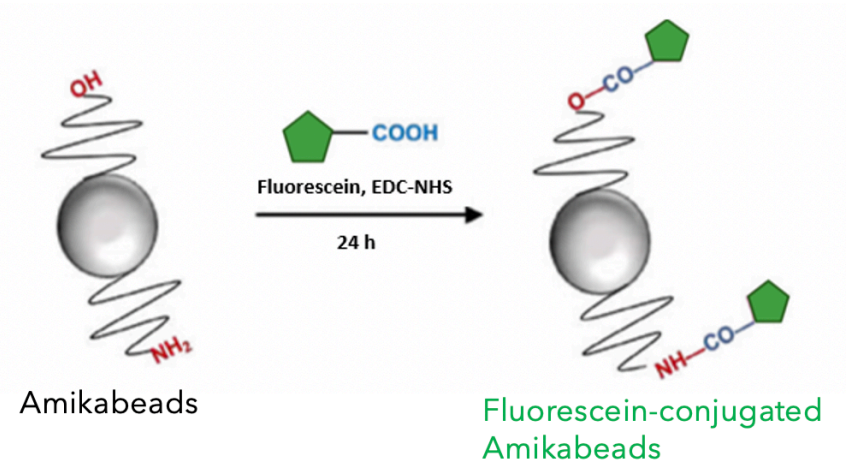


Fig. 22. Fluorescein-conjugated Amikabeads. Schematic of the conjugation of Amikabeads with Fluorescein using EDC-NHS. (*Rho-conjugated Amikabeads were procured from Mr. Subhadeep Dutta, doctoral student, Rege Bioengineering Laboratory, figure credits: Mr. Subhadeep Dutta)*

3.9 Fluorescence Intensity Optimization

An investigation of the preliminary visualization studies on Fluorescein-conjugated Amikabeads revealed the high fluorescence intensity shown by the label, leading to poor image quality and difficulty in differentiating between encapsulated layer and spheroid. To terminate this issue, Amikabeads were conjugated with Fluorescein and six serial dilutions of the stock dispersion (10 mg/mL) were made – 2X, 5X, 10X, 20X, 50X, 100X – in DMEM. The fluorescence intensity of each dilution was measured (**Table 9**) using a plate reader and plotted against the respective concentration (**Fig. 23A**). Confocal images of each serial dilution at 0.75 zoom using a 10X objective lens pointed towards the concentration of 0.1 mg/mL or 100X dilution displaying the optimum intensity to differentiate between each Amikabead on different focal planes (**Fig. 23B**).

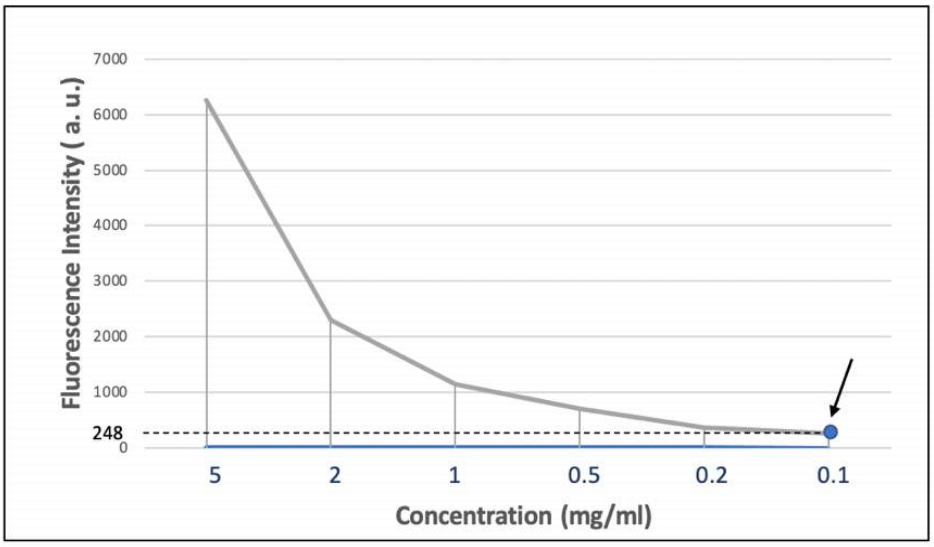
Further encapsulation experiments with Fluorescein-conjugated Amikabeads were performed after ensuring the fluorescence intensity of the solution to be 248 arbitrary units (a.u.) using a plate reader.

Table 9. Fluorescence Intensity of each serial dilution of Fluorescein-conjugated Amikabeads

Fluorescence Intensity

Concentration	Fluorescence Intensity (a.u.)
2X (5 mg/mL)	6268
5X (2 mg/mL	2297
10X (1 mg/mL)	1142
20X (0.5 mg/mL)	705
50X (0.2 mg/mL)	357
100X (0.1 mg/mL)	**<u>248</u>**

A.



B.

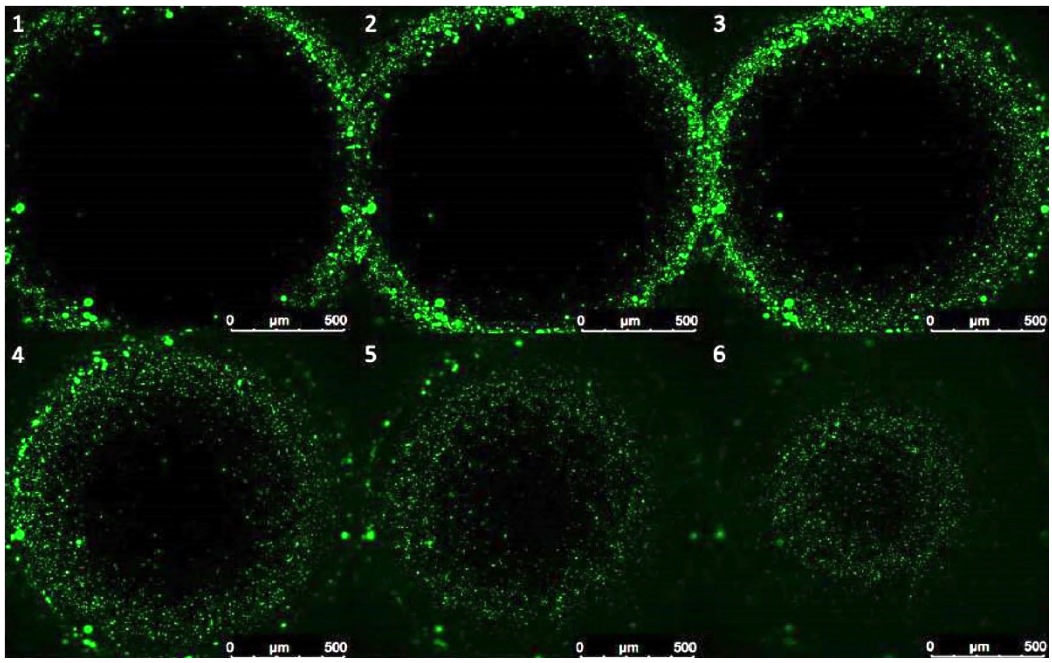


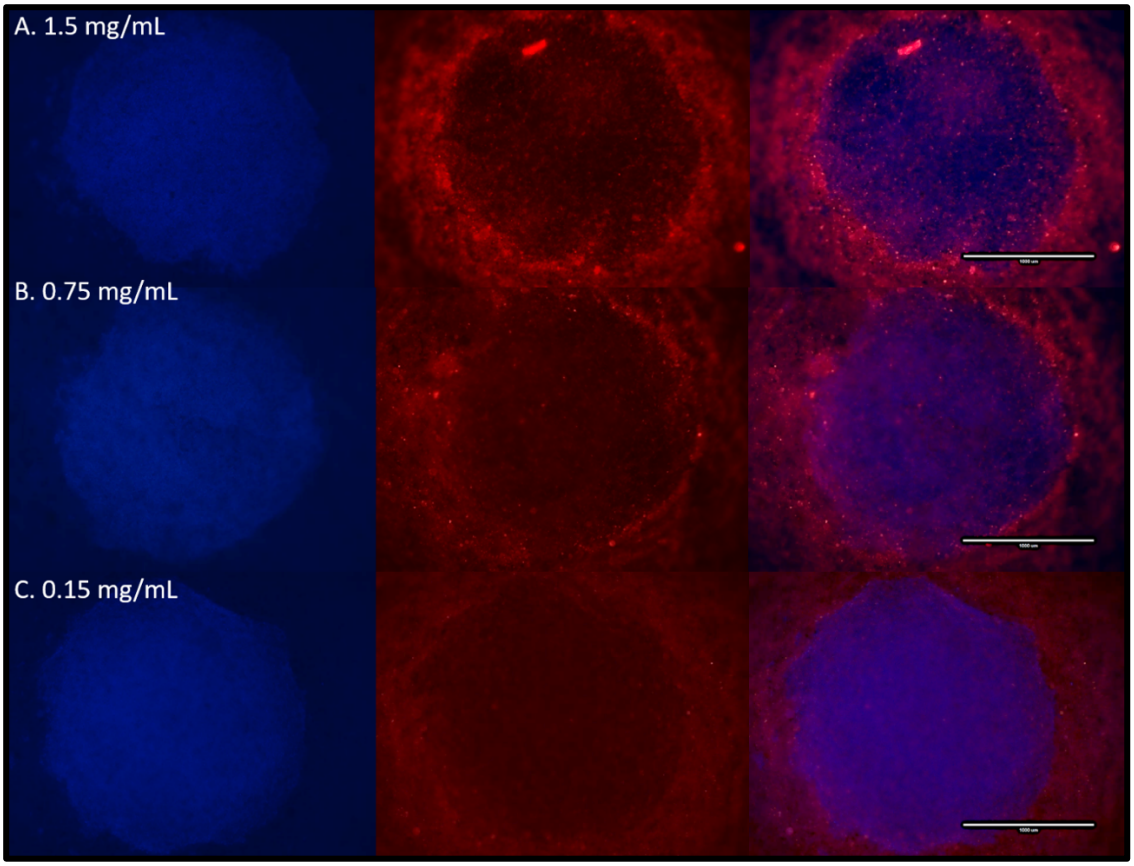
Fig. 23. Intensity optimization of Fluorescein-conjugated Amikabeads. Fluorescence intensity plots of serial dilutions of Fluorescein-conjugated Amikabeads. Optimum intensity was observed at 248 a.u. of the Amikabead dispersion (marked by a black arrow). B. Confocal images of an A375 spheroid (initial cell density = 30,000 cells/well) encapsulated in 0.1 mg/mL of *low* Amikabead dispersion. The images represent 6 sections of 5 µm each from middle of spheroid (1) to bottom of spheroid (6) completely encapsulated with Amikabeads (in green), as evident by the strong fluorescent signal. Objective: 10X, Scale = 500 µm. *(Images acquired in collaboration with Mr. Rajeshwar Nitiyanandan, doctoral student in Rege Bioengineering Laboratory and Ms. Page Baluch, Research Scientist, W. M. Keck Bioimaging Laboratory in the School of Life Sciences, ASU)*

3.10 Visualization of the Encapsulated Tumor Spheroids

Fluorescence microscopy. Confocal fluorescence microscopy was employed to visualize the entrapment of spheroids generated on polystyrene 96 well cell culture plates in fluorescently labeled spheroids. As shown in **Fig. 24A-D**, DAPI stained T-47D spheroids (initial cell density = 30,000 cells/well, ~ 1000 µm) portrayed visibly compact layers of Rho-conjugated Amikabeads of concentration 1.5 mg/mL, 0.75 mg/mL, 0.15 mg/mL

around them when imaged using a 10X Objective on the EVOS FL Auto Live Cell Imaging Inverted Microscope System. A blue contrast from the spheroid was demonstrated with red from the Amikabeads. This study acted as one of the preliminary checkpoints of successful encapsulation of spheroids with Amikabeads.

RHODAMINE-CONJUGATED AMIKABEADS + T-47D SPHEROID



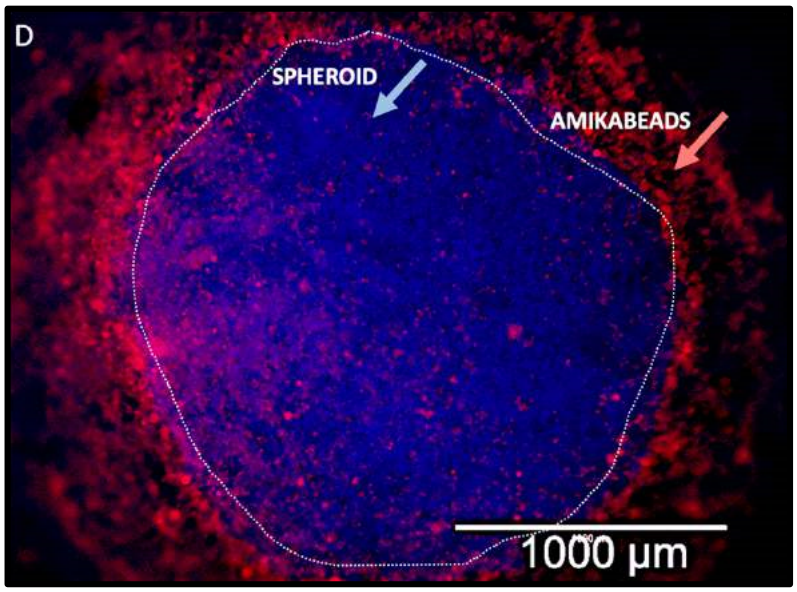


Fig. 24. Fluorescence microscopy images of encapsulated T-47D spheroid. T-47D spheroids (initial cell density = 30,000 cells/well) visualized on a polystyrene 96 well cell culture plate with a standard 10X objective at an analyzable depth of approximately 100 µm. Fluorescence microscopy images of T-47D spheroids stained with 5 µL DAPI/well (in blue) encapsulated in a compact layer of Rho-conjugated spheroids of concentration A. 1.5 mg/mL, B. 0.75 mg/mL, and C. 0.15 mg/mL. D. A distinctive boundary (marked with white dots) between T-47D spheroid (marked with a blue arrow) encapsulated in 0.75 mg/mL Amikabeads (marked with a red arrow) while focusing on the middle of the spheroid. Scale = 1000 µm. *(Images acquired in collaboration with Mr. Rajeshwar Nitiyanandan, doctoral student in Rege Bioengineering Laboratory)*

Laser scanning confocal microscopy of DAPI-Rho models. Confocal z-stacks were acquired and analyzed to evaluate the total and positional fluorescent signal for T-47D spheroids (initial cell density = 30,000 cells/well) generated on 96 well glass-bottomed plates labeled with DAPI and encapsulated with Rho-conjugated Amikabeads.

As demonstrated in **Fig. 25**, imaging was performed by capturing a series of horizontal scans through the spheroids using Leica Digital Light Sheet with a Hamamatsu Orca Flash 4.0 V2 CMOS camera. The serial images were arranged as a vertical stack/z-stack using HyVo2 Deconvolution software – SVI Huygens integrated. Each optical section was

acquired at 5 μm interval, with a typical imaging stack consisting of 30 to 40 optical sections per spheroid.

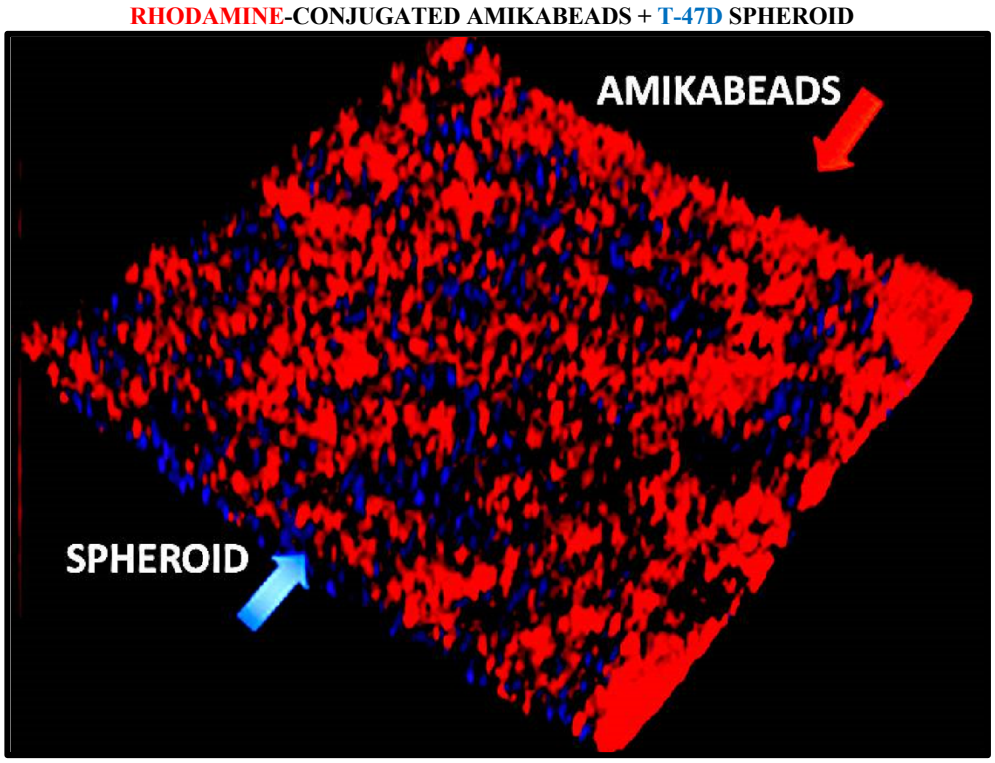


Fig. 25. Z-stack projection of encapsulated T-47D spheroid. Z-stack of a T-47D spheroid (initial cell density = 30,000 cells/well) stained with 5 μL DAPI/well encapsulated in 0.75 mg/mL Rho-conjugated Amikabeads imaged using a Light Sheet Confocal Microscope. *(Images acquired in collaboration with Mr. Rajeshwar Nitiyanandan, doctoral student in Rege Bioengineering Laboratory)*

In recent years, confocal microscopy in combination with 3D models has been commonly used to study morphologies.[68] For the encapsulated T-47D spheroids, 3D reconstruction per stack was performed to visualize the encapsulation on different spots as illustrated in **Fig. 26**. Image size was 2048 x 2048 pixels. These projections were especially useful in visualizing the 3D microenvironment of the encapsulated spheroid (hereafter, *model*).

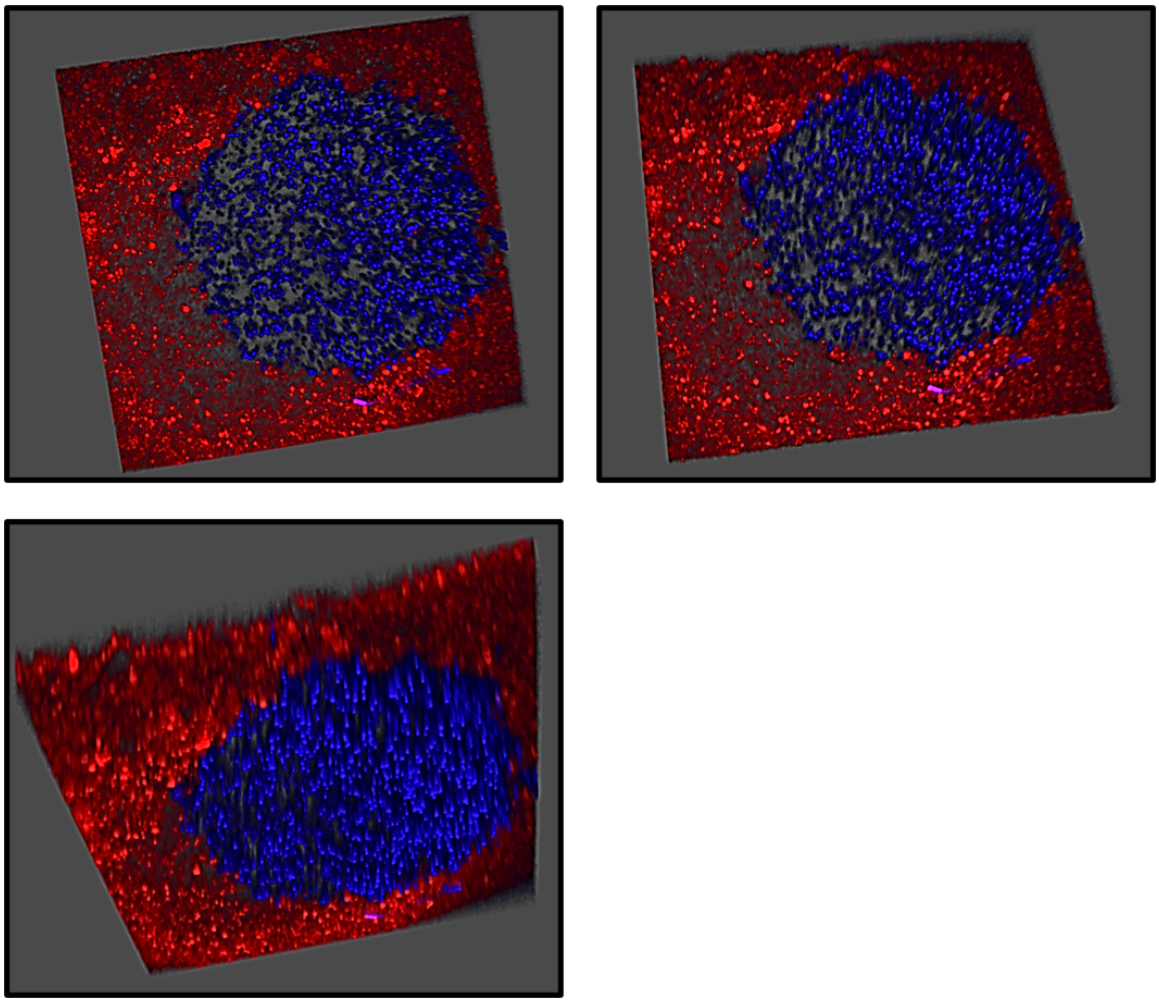


Fig. 26. 3D projections of Z-stacks of encapsulated T-47D spheroids. 3D projections of z-stacks of confocal microscopy images captured from a T-47D spheroid stained with DAPI (in blue) encapsulated in 0.75 mg/mL Rho-conjugated Amikabeads (in red). Total depth of the stack was 200 µm from the bottom and each section was 5 µm. *(Images acquired in collaboration with Mr. Rajeshwar Nitiyanandan, doctoral student in Rege Bioengineering Laboratory)*

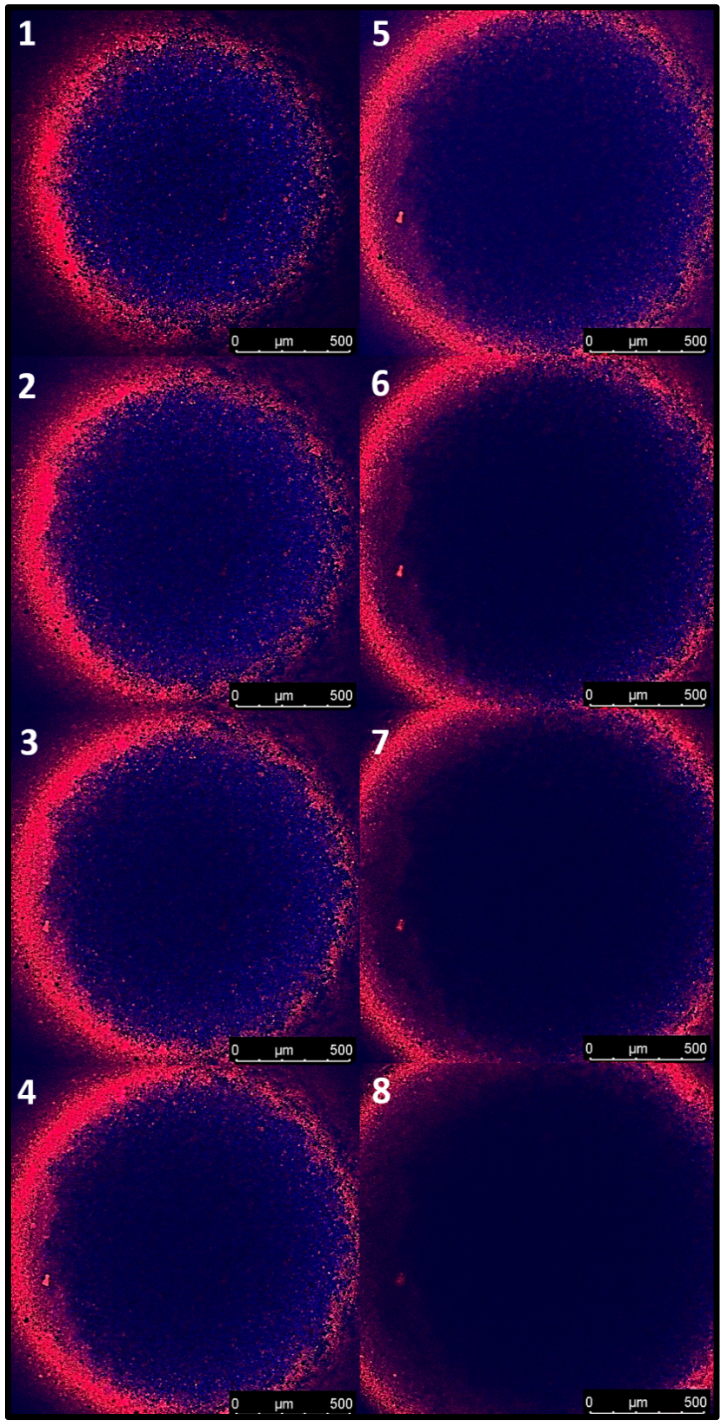
Laser scanning confocal microscopy of Hoechst-Rho models. A375 spheroids were generated using initial cell density of 30,000 cells/well and encapsulated in Rho-conjugated Amikabeads. The spheroids were then stained with Hoechst 33342 and visualized in the same way as mentioned above. Nuclear staining with 0.5 µL/well Hoechst

demonstrated higher quality images than using DAPI and was used in further experiments (**Fig. 27**).

Laser scanning confocal microscopy of DRAQ5™-Fluorescein models. As discussed above, A375 spheroids were generated using initial cell density of 30,000 cells/well and encapsulated in Fluorescein-conjugated Amikabeads with concentration 0.1 mg/mL. The spheroids were then stained with DRAQ5™ and visualized using laser scanning confocal microscopy. The images demonstrated less contrast than the Hoechst-Rho model due to overlap of red fluorescence signal from the spheroids and the green fluorescence signal from the Amikabeads. Although, an overall encapsulation of the spheroid was verified, as demonstrated in **Fig. 28**.

RHODAMINE-CONUGATED AMIKABEADS + A375 SPHEROID

A.



B.

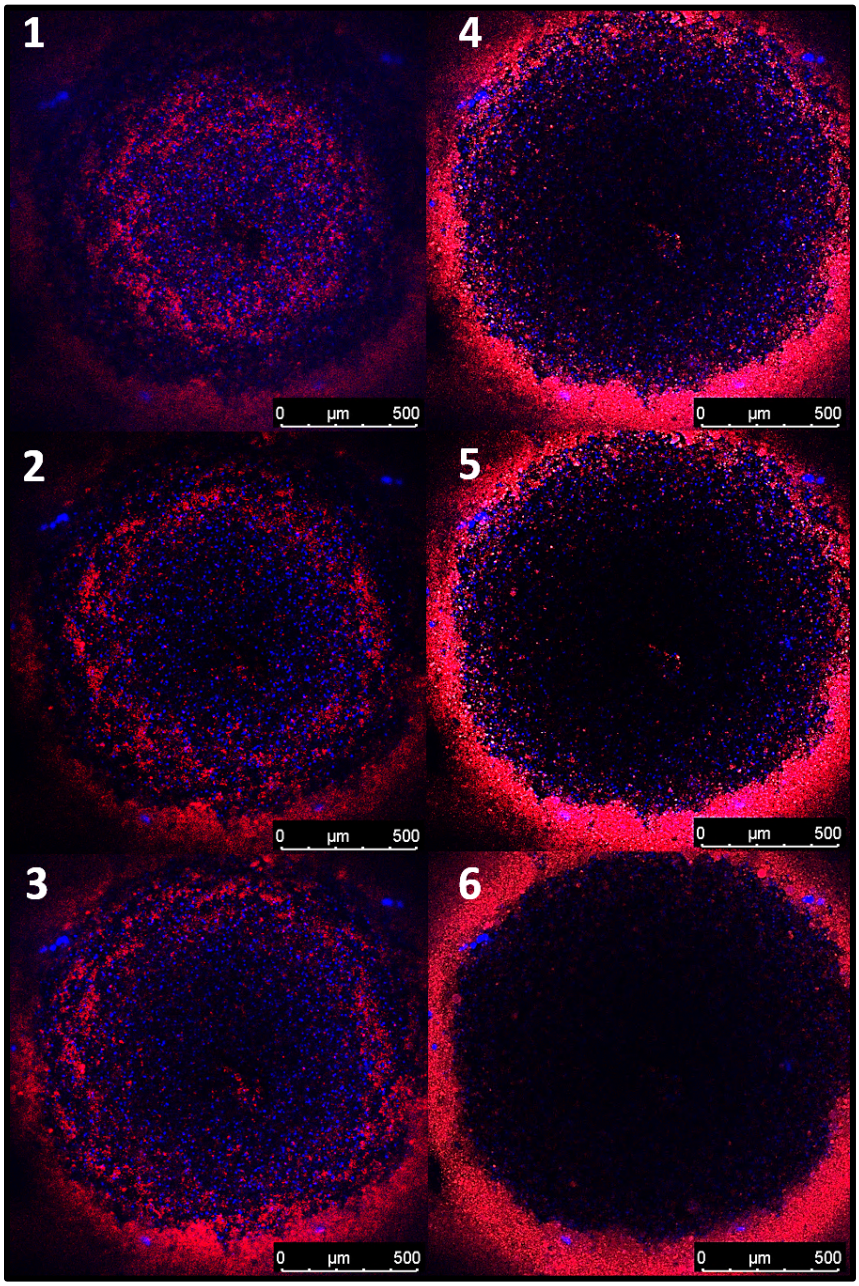


Fig. 27. **Confocal Microscopy images of encapsulated A375 spheroids.** A375 spheroid model (initial cell density = 30,000 cells/well, Rho- conjugated Amikabeads concentration = A. 0.75 mg/mL, B. 0.15 mg/mL) with Hoechst 33342 as nuclear stain visualized using a laser scanning confocal microscope and a standard 10X objective with a zoom of 0.75. The images illustrate sections of 5 µm each from the bottom of the spheroid denoted by 1 to the middle of the spheroid. The prominent spherical boundary between spheroid (in blue) and Amikabeads layer (in red) attests to the overall coverage of the spheroid in Amikabeads. Scale = 500 µm.

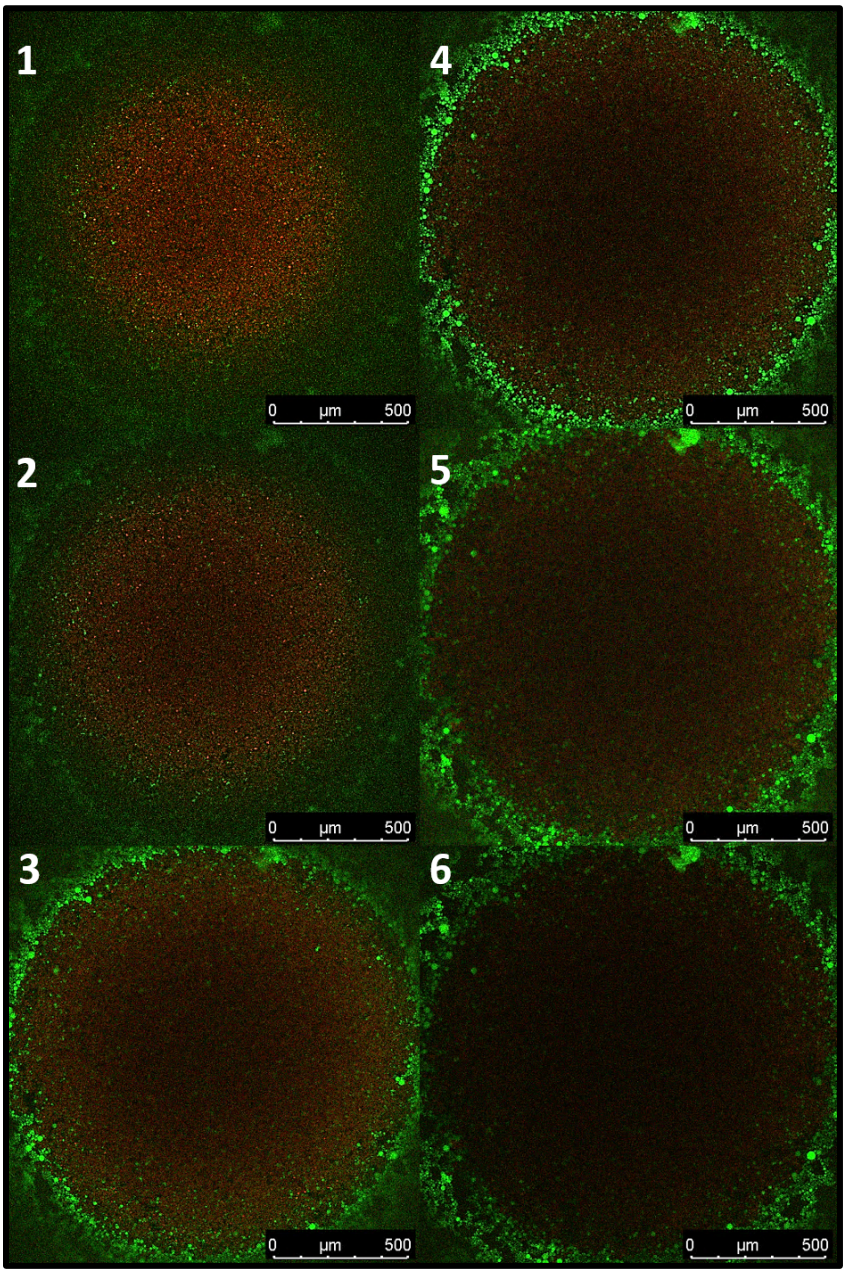
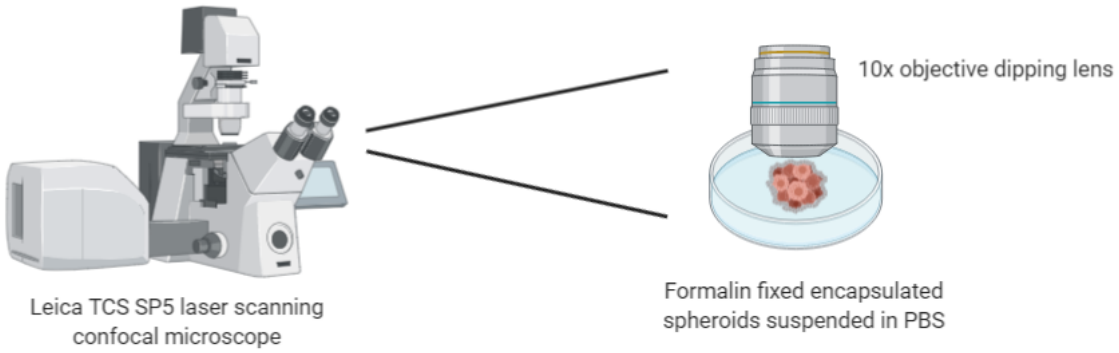


Fig. 28. **Confocal microscopy images of A375 spheroids encapsulated with Fluorescein-conjugated Amikabeads.** A375 spheroid model (initial cell density = 30,000 cells/well, Fluorescein- conjugated Amikabeads concentration = 0.1 mg/mL) with DRAQ5™ as nuclear stain visualized using a laser scanning confocal microscope and a standard 10X objective with a zoom of 0.75. The images illustrate 6 sections of 5 µm each from the bottom of the spheroid (1) to the middle of the spheroid (6). The prominent spherical boundary between spheroid (in red) and Amikabeads layer (in green) attests to the overall coverage of the spheroid in Amikabeads. Scale = 500 µm.

Dipping lens confocal microscopy. To study full depth images of models, dipping lens confocal microscopy was performed using Leica SP5 AOBS Spectral Confocal microscope with a 200-degree field rotation and pixel resolution of up to 8000 x 8000, as shown in **Fig. 29A**. A375 spheroids with initial cell density of 30,000 cells/well encapsulated with Rho-conjugated Amikabeads were fixed with 10% NBF overnight. The fixed spheroids were removed from the wells and suspended in 1X PBS in a clear petri dish. The sample was placed on the stage and imaged using 10X objective dipping lens. The multi-dimensional image series were acquired and analyzed using Leica Confocal Software (LSC). The images captured through dipping lens aligned with those captured using confocal microscope in terms of a spherical boundary of Amikabeads seen around the spheroid even after washing and fixing the encapsulated spheroid, as demonstrated in **Fig. 29B-C**.

A.



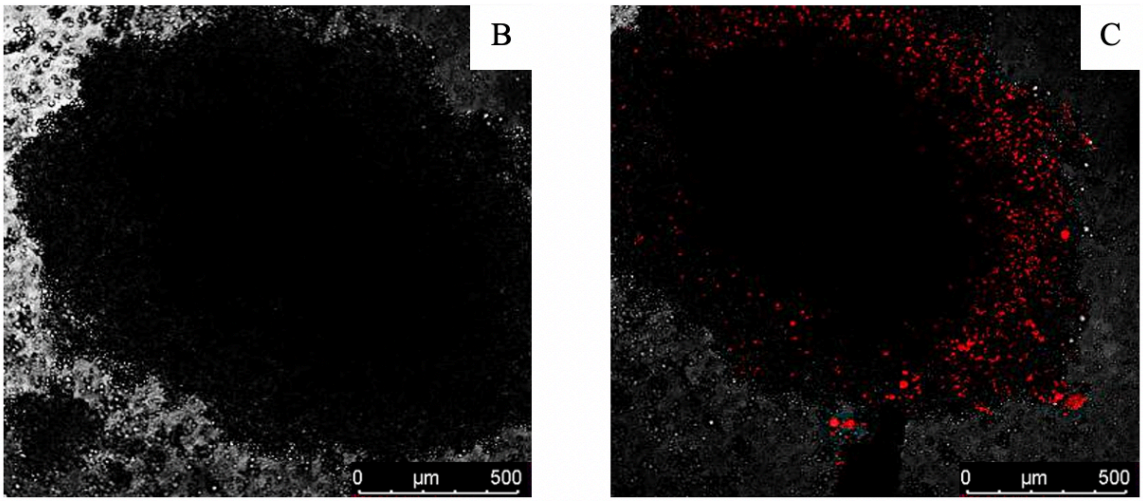


Fig. 29. **Dipping lens confocal microscopy of encapsulated A375 spheroids.** A. Bright field image, B. Confocal microscopy image demonstrating the encapsulation of an A375 spheroid (dark) in 0.75 mg/mL Rho-conjugated Amikabeads (in red) using a 10X objective dipping lens. Scale = 500 µm. *(Images acquired in collaboration with Mr. Rajeshwar Nitiyanandan, doctoral student in Rege Bioengineering Laboratory and Ms. Page Baluch, Research Scientist, W. M. Keck Bioimaging Laboratory in the School of Life Sciences, ASU)*

3.11 Visualization of Encapsulated hMSC Models

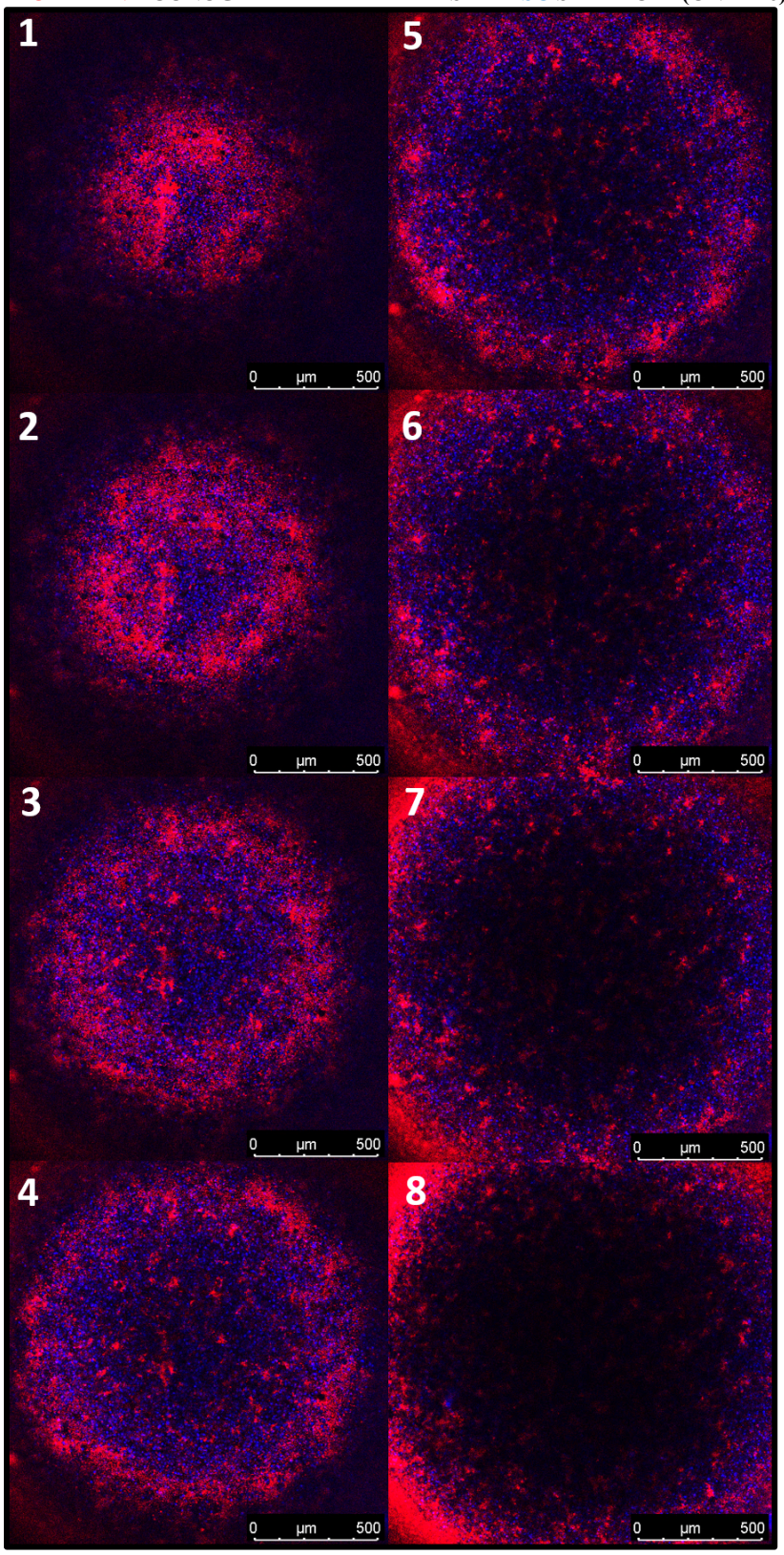
Laser scanning confocal microscopy of Hoechst-Rho models. Hoechst stained A375 spheroids revealed exceedingly high-quality images of the contrast between them and the Amikabeads layer. The same combination was tried with hMSC spheroids of initial cell density 30,000 cells/well cultured on AM6 and AM7 and encapsulated with 0.75 mg/mL (**Fig. 30A-B**) and 0.15 mg/mL (**Fig. 31A-B**) concentrations of Rho-conjugated Amikabeads. The images captured using 10X objective at 0.75 zoom demonstrated comprehensive coverage of the spheroid from bottom to top for both the concentrations. It was observed that encapsulation with 0.75 mg/mL Amikabead dispersion exhibited a stronger red fluorescence signal and more spheroid coverage than with 0.15 mg/mL, which

exhibited a more homogeneous wrapping of spheroid with the Amikabeads but a signal of comparatively lower intensity.

Laser scanning confocal microscopy of DRAQ5™-Fluorescein models. hMSC spheroids generated on AM6 and AM7 coated cell culture plates were stained with DRAQ5™ and encapsulated in 0.1 mg/mL Fluorescein-conjugated Amikabeads, followed by confocal microscopy using a 10X objective. Both spheroids showed identical encapsulation – a clear boundary visible between spheroid and Amikabeads layer, evidencing the compact packing of Amikabeads around the spheroids potentially due to interactions with cell surface. The overlap of fluorescent signals from Amikabeads encapsulating the bottom surface of the spheroid with the nuclear stain demonstrated an orange tinge in the middle, as illustrated in **Fig. 31C**.

RHODAMINE-CONUGATED AMIKABEADS + hMSC SPHEROID (ON AM6)

A.



B.

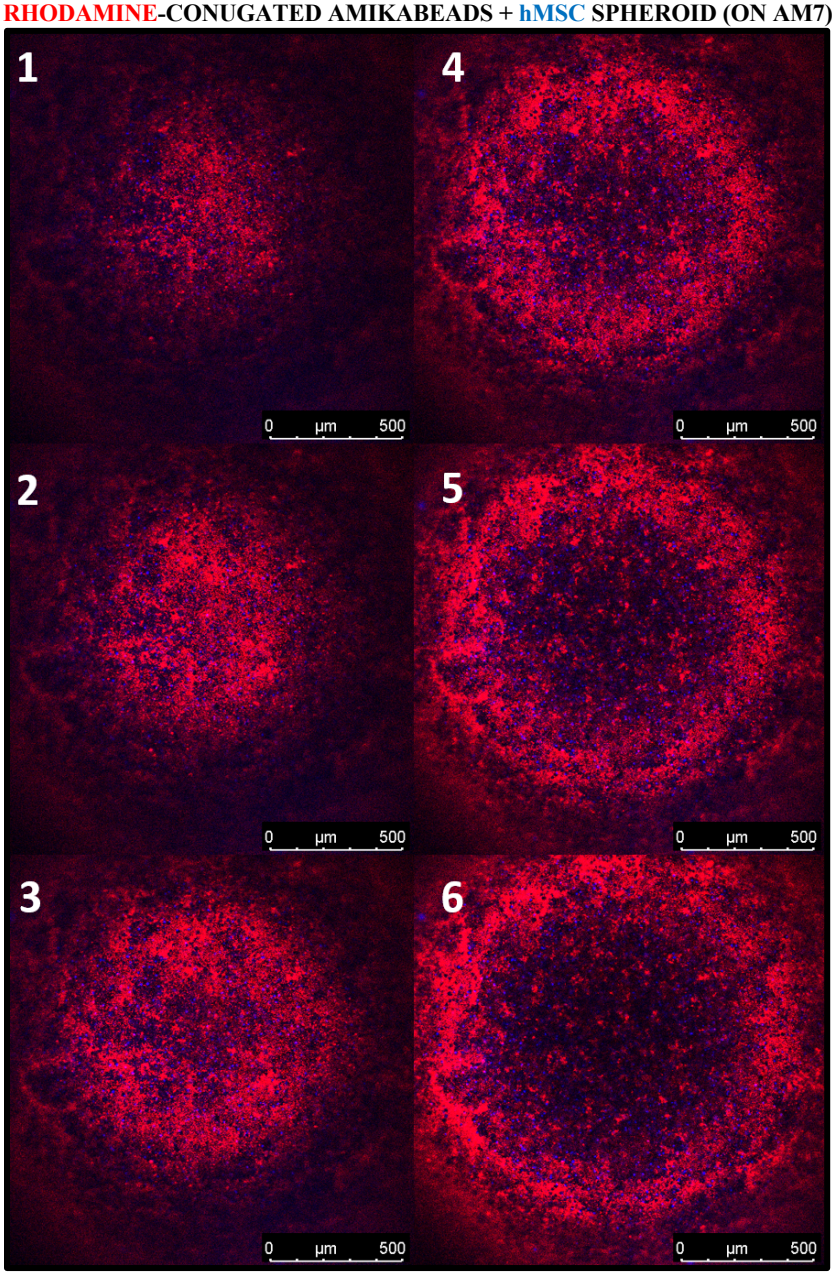
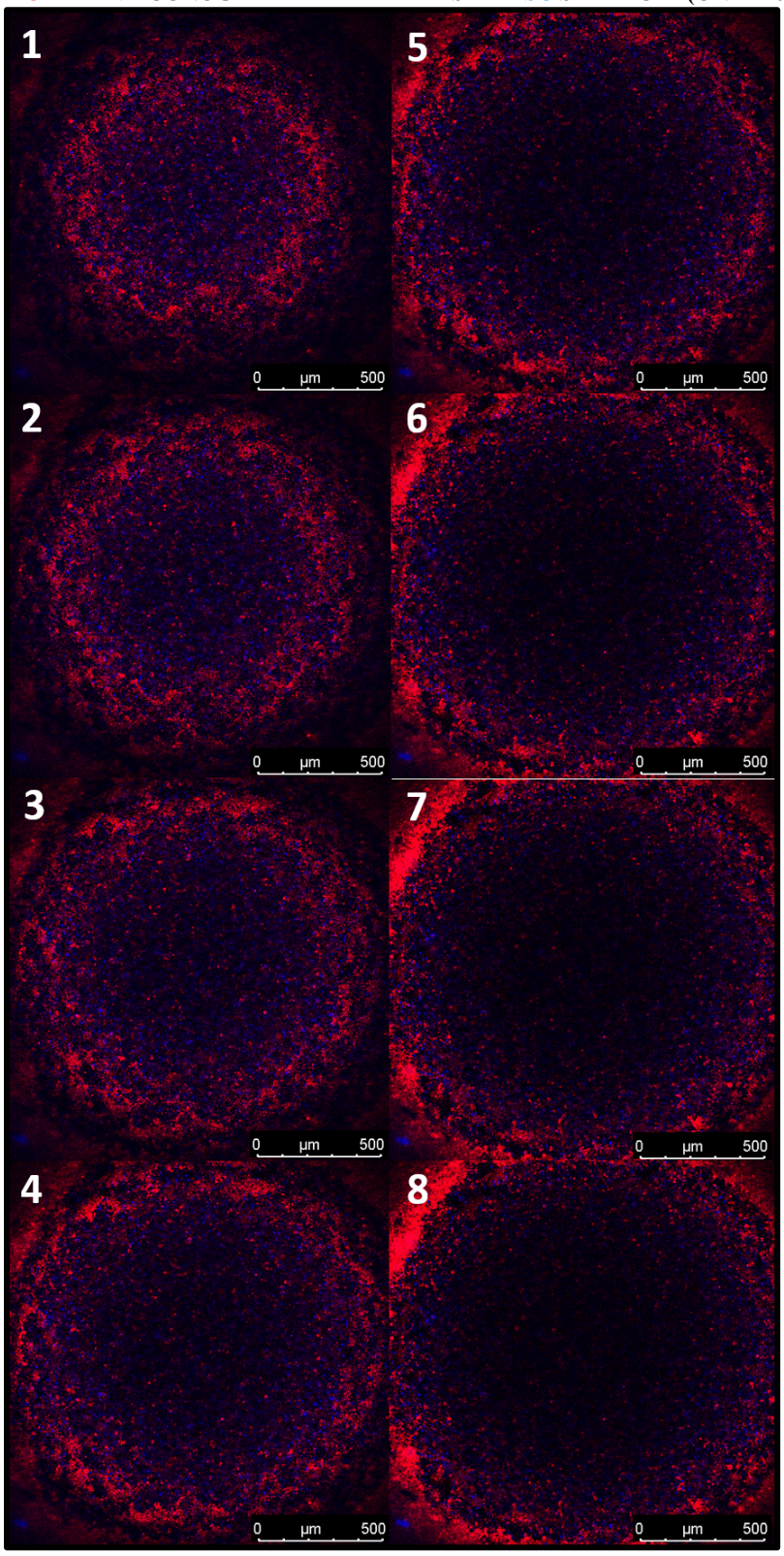


Fig. 30. Encapsulated hMSC spheroids. hMSC spheroid model (initial cell density = 30,000 cells/well cultured on A. AM7, B. AM6, Rho- conjugated Amikabeads concentration = 0.75 mg/mL) with Hoechst 33342 as nuclear stain visualized using a laser scanning confocal microscope and a standard 10X objective with a zoom of 0.75. The images illustrate sections of 5 µm each from the bottom of the spheroid (1) to the middle of the spheroid (A. 6, B. 8). The prominent spherical boundary between spheroid (in blue) and Amikabeads layer (in red) attests to the overall coverage of the spheroid in Amikabeads. Scale = 500 µm.

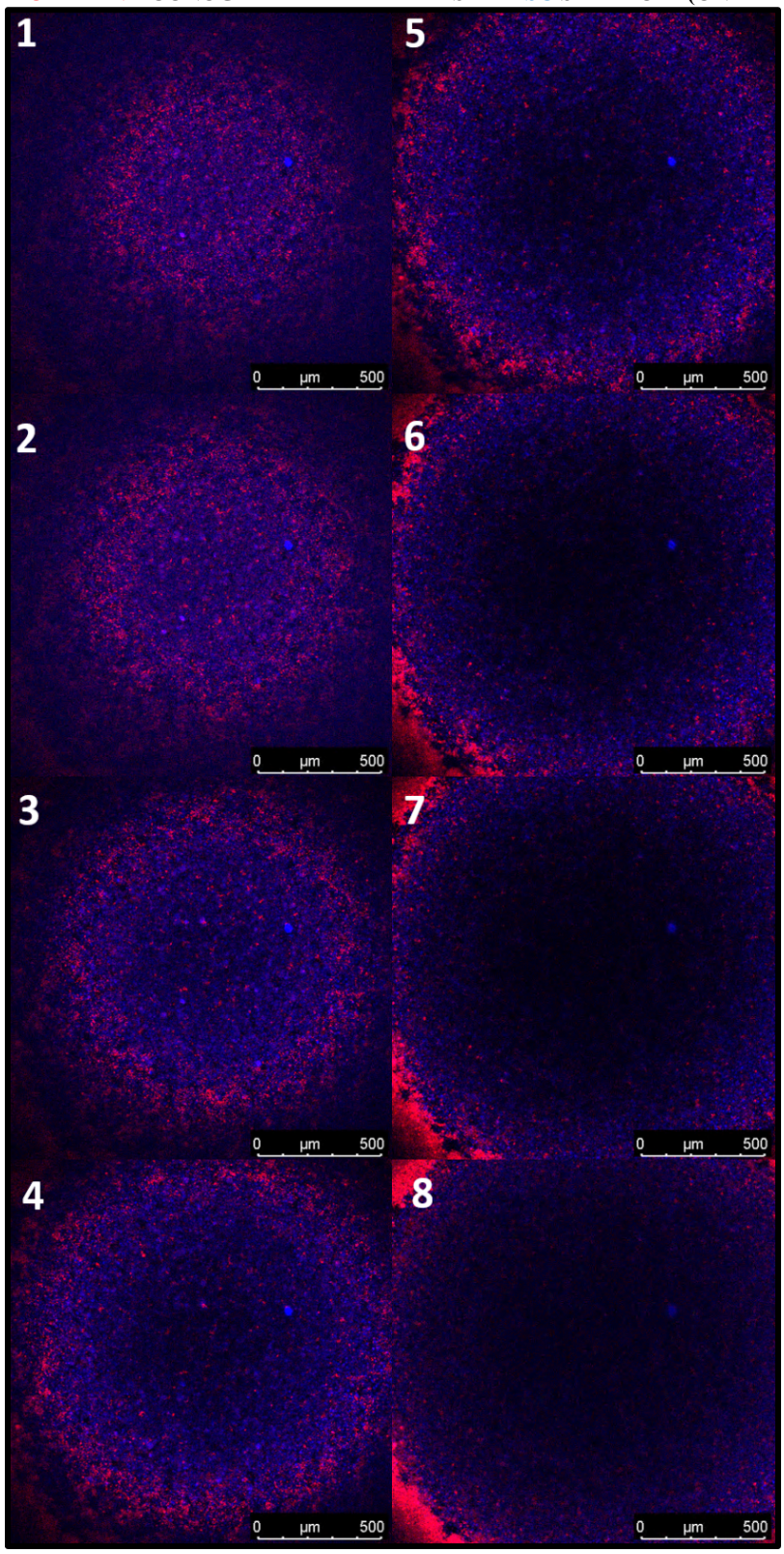
RHODAMINE-CONUGATED AMIKABEADS + hMSC SPHEROID (ON AM6)

A.



RHODAMINE-CONUGATED AMIKABEADS + hMSC SPHEROID (ON AM7)

B.



C.

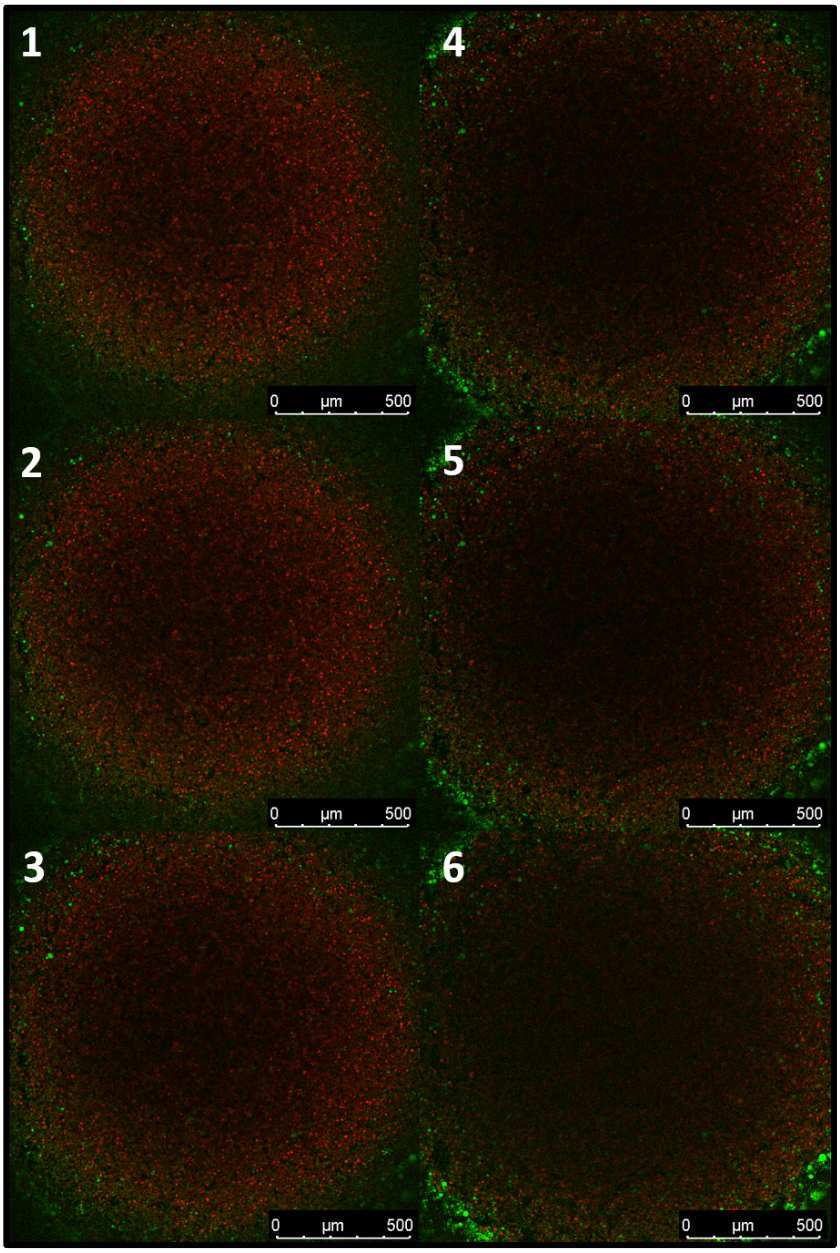
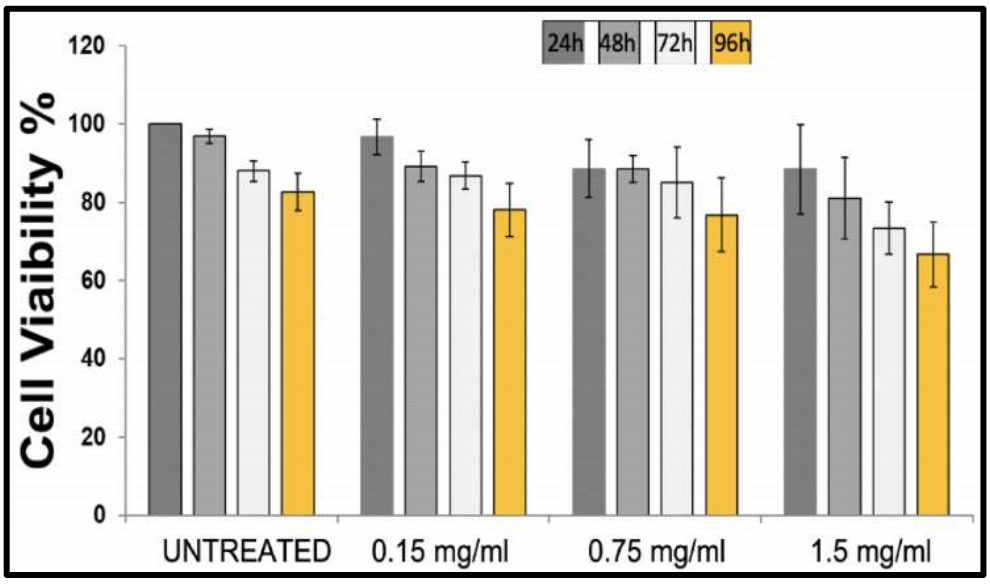


Fig. 31. **Encapsulated hMSC spheroids.** hMSC spheroid model (initial cell density = 30,000 cells/well cultured on A. AM7, B. AM6, Rho-conjugated Amikabeads concentration = 0.15 mg/mL) with Hoechst 33342 as nuclear stain. C. hMSC spheroid model (initial cell density = 30,000 cells/well cultured on AM6, Fluorescein-conjugated Amikabeads concentration = 0.1 mg/mL) with DRAQ5^{TM} as nuclear stain. The models were visualized using a laser scanning confocal microscope and a standard 10X objective with a zoom of 0.75. The images illustrate sections of 5 µm each from the bottom of the spheroid (1) to the middle of the spheroid (A. 6, B. 8, C. 6). The prominent contrast between spherical boundary of spheroids and Amikabeads layer attests to the overall coverage of the spheroid in Amikabeads. Scale = 500 µm.

3.12 Cell Viability Assay

Toxicity studies using CellTiter-Glo assay were carried out to test the viability of cells in the A375 spheroid following encapsulation with Amikabeads. The outcomes indicated ~85% cell viability in the spheroids encapsulated with Amikabeads-P and ~80% cell viability in the spheroids encapsulated with Amikabeads-Q at 72 hours at an identical concentration of .75 mg/mL of the Amikabeads, as demonstrated in **Fig. 32A-B**. Further studies with Flow Cytometry to analyze the cell cycle were performed to confirm the cell viability post encapsulation.

A.



B.

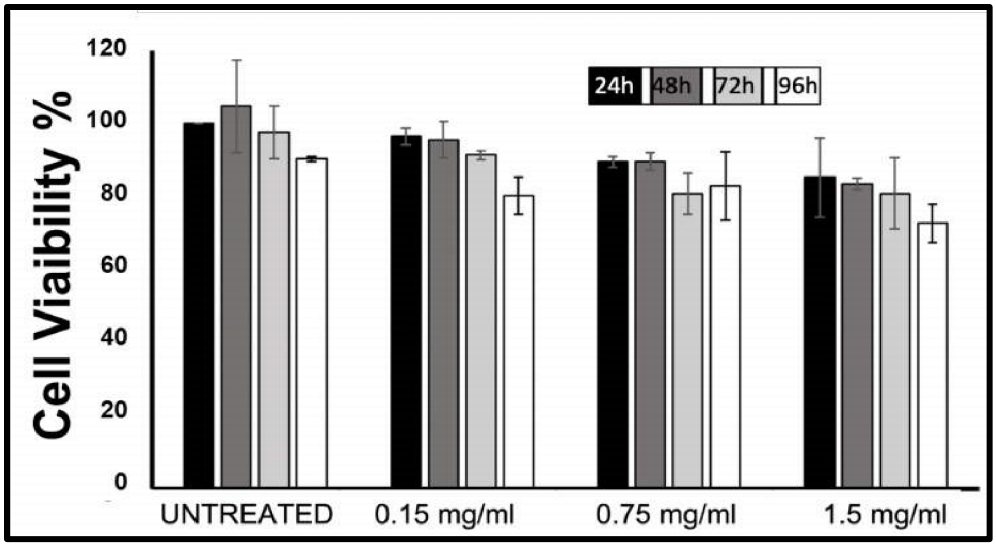


Fig. 32. **Cell viability assay.** Cell viability studies through CellTiter-Glo assay indicating A. ~85% cell viability in A375 spheroids encapsulated with Amikabeads-P B. ~80% cell viability in spheroids encapsulated with Amikabeads-Q at a concentration of 0.75mg/ml after 72 hours. *(Analyses were performed in collaboration with Mr. Rajeshwar Nitiyanandan, doctoral student in Rege Bioengineering Laboratory)*

3.13 Flow Cytometry *(study still in progress)*

Currently, the cell viability analysis of 3D fluorescence stained spheroids relies on cytotoxicity assays, such as described in Section 3.13, but they are often unreliable due to the morphological change within the spheroids.[69] Techniques like microscopy were time consuming and provided low throughput. Therefore, to analyze the behaviors of cells in the spheroids and provide accurate statistical information about individual cells, cell cycle analysis was performed using flow cytometry. This technique has high-speed and throughput capabilities and therefore, has garnered popularity to study characteristics of single cells as they flow in a fluid stream through a beam of light.[70]

A375 models were dissociated along with Amikabeads only and Amikabeads + 2D cells controls and stained with 1X PBS:Triton X:Propidium Iodide at a ratio of 10:1:1 (v/v/v). Cell cycle analysis was performed at appropriate parameters on FACSAria Ilu Cell Sorter.

CHAPTER 4

CONCLUSIONS

3D microenvironment is the natural state of growth for the cells where their interactions affect their proliferation, differentiation, and morphology.[71,72] This multi-dimensional system can resolve limitations of monolayer cultures and mimic the behavior of cells in vivo. 3D tumor and stem cell cultures have shown applicability in various regenerative medicine fields such as tissue engineering and organoid production as well as cancer research. In this project, 3D spheroids of T-47D, A375, and hMSC cell lines were engineered and encapsulated in Amikabeads for their potential use in loading and proximal delivery of bioactive compounds and drugs. Robust spheroid formation was demonstrated by extensive and sophisticated microscopic techniques. Overall coverage of spheroids in Amikabeads, possibly due to charge interactions, was also demonstrated. The cells exhibited approximately 80% viability through cytotoxicity assays. In future, the application of Amikagel as a platform technology to generate encapsulated spheroid models could significantly advance its place in the current matrices used for spheroid synthesis. Investigation of these models for applicability in tissue engineering, specifically to study the delivery of bioactive compounds loaded into Amikabeads to the cells, could advance their use in disease modeling, drug screening, and regenerative medicine.

CHAPTER 5

FUTURE DIRECTIONS

Future work for the applicability of 3D encapsulated models of tumor and stem cell spheroids include the following:

1. Ongoing flow cytometry analyses with appropriate 2D and Amikabeads controls to analyze the percentage of cell populations in encapsulated spheroids in various cell cycle phases.
2. Generation of A375 and hMSC spheroids with initial cell density of 10^6 cells/well in 24-well Amikagel coated cell culture plates and their visualization using paraffin embedding and H&E staining.
3. Loading bioactive compounds, such as drugs, growth factors in Amikabeads and using them to encapsulate the spheroid to observe proximal delivery over time, as shown in **Fig. 33**.

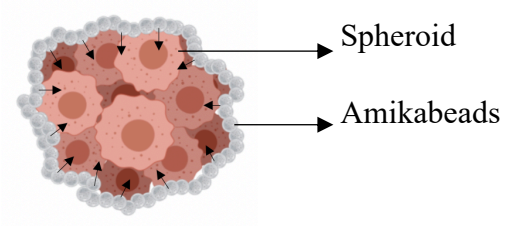


Fig. 33. Proximal delivery of bioactive compounds. Bioactive compounds such as nuclear stains can be loaded into Amikabeads and their delivery to spheroids can be observed over time.

4. Engineering multicellular constructs using co-culture of cells and Amikabeads in different layers, as shown in **Fig. 34**.

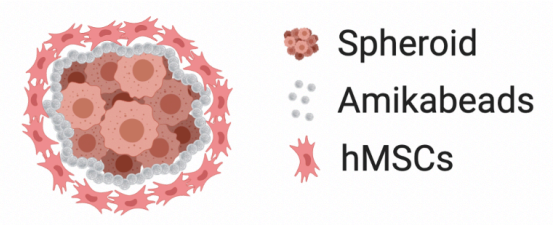


Fig. 34. Multicellular constructs using spheroid and Amikabeads. Multicellular constructs of tumor spheroid, Amikabeads, and hMSCs can be engineered to study the interactions of tumor cells with other cell lines and their cellular progression.

REFERENCES

1. Harrison, R. G. The developing nerve. *read before the Society for Experimental Biology and Medicine* (1907).

2. Breslin, S. & O'Driscoll, L. Three-dimensional cell culture: the missing link in drug discovery. *Drug Discov Today* **18**, 240–249 (2013).

3. Lv, D., Hu, Z., Lu, L., Lu, H. & Xu, X. Three-dimensional cell culture: A powerful tool in tumor research and drug discovery. *Oncol Lett* **14**, 6999–7010 (2017).

4. Weigelt, B., Ghajar, C. M. & Bissell, M. J. The need for complex 3D culture models to unravel novel pathways and identify accurate biomarkers in breast cancer. *Adv Drug Deliver Rev* **69**, 42–51 (2014).

5. Abbott, A. Biology's new dimension. *Nature* 870–872 (2003).

6. Qutub, A. A. & Popel, A. S. Elongation, proliferation & migration differentiate endothelial cell phenotypes and determine capillary sprouting. *Bmc Syst Biol* **3**, 13 (2009).

7. Ayala, P., Lopez, J. I. & Desai, T. A. Microtopographical Cues in 3D Attenuate Fibrotic Phenotype and Extracellular Matrix Deposition: Implications for Tissue Regeneration. *Tissue Eng Pt A* **16**, 2519–2527 (2010).

8. Li *et al.* Survival advantages of multicellular spheroids vs. monolayers of HepG2 cells in vitro. *Oncol Rep* **20**, 1465–1471 (1994).

9. Adelöw, C., Segura, T., Hubbell, J. A. & Frey, P. The effect of enzymatically degradable poly(ethylene glycol) hydrogels on smooth muscle cell phenotype. *Biomaterials* **29**, 314–326 (2008).

10. Chang, T. T. & Hughes-Fulford, M. Monolayer and Spheroid Culture of Human Liver Hepatocellular Carcinoma Cell Line Cells Demonstrate Distinct Global Gene Expression Patterns and Functional Phenotypes. 559–567 (2009).

11. Jacks, T. & Weinberg, R. A. Taking the Study of Cancer Cell Survival to a New Dimension. *Cell* **111**, 923–925 (2002).

12. Trevino, A. E. *et al.* Chromatin accessibility dynamics in a model of human forebrain development. *Science* **367**, eaay1645 (2020).

13. Pașca, S. P. The rise of three-dimensional human brain cultures. *Nature* **553**, 437–445 (2018).

14. WÄSTFELT, M., FADEEL, B. & HENTER, J. -I. A journey of hope: lessons learned from studies on rare diseases and orphan drugs. *J Intern Med* **260**, 1–10 (2006).

15. J.Bissell, M., C.Radisky, D., Rizki, A., M.Weaver, V. & W.Petersen, O. The organizing principle: microenvironmental influences in the normal and malignant breast. *Differentiation* **70**, 537–546 (2002).

16. Lin, R.-Z., Chou, L.-F., Chien, C.-C. M. & Chang, H.-Y. Dynamic analysis of hepatoma spheroid formation: roles of E-cadherin and β1-integrin. *Cell Tissue Res* **324**, 411–422 (2006).

17. Hu, G. & Li, D. Three-dimensional modeling of transport of nutrients for multicellular tumor spheroid culture in a microchannel. *Biomed Microdevices* **9**, 315–323 (2007).

18. Curcio, E. *et al.* Mass transfer and metabolic reactions in hepatocyte spheroids cultured in rotating wall gas-permeable membrane system. *Biomaterials* **28**, 5487–5497 (2007).

19. Jiang, Y., Pjesivac-Grbovic, J., Cantrell, C. & Freyer, J. P. A Multiscale Model for Avascular Tumor Growth. *Biophys J* **89**, 3884–3894 (2005).

20. Carlsson, J. & Acker, H. Relations between ph, oxygen partial pressure and growth in cultured cell spheroids. *Int J Cancer* **42**, 715–720 (1988).

21. Mueller-Klieser, W. Method for the determination of oxygen consumption rates and diffusion coefficients in multicellular spheroids. *Biophys J* **46**, 343–348 (1984).

22. Place, E. S., George, J. H., Williams, C. K. & Stevens, M. M. Synthetic polymer scaffolds for tissue engineering. *Chem Soc Rev* **38**, 1139–1151 (2009).

23. Lin, R.-Z., Lin, R.-Z. & Chang, H.-Y. Recent advances in three-dimensional multicellular spheroid culture for biomedical research. *Biotechnol J* **3**, 1172–1184 (2008).

24. Ivascu, A. & Kubbies, M. Rapid Generation of Single-Tumor Spheroids for High-Throughput Cell Function and Toxicity Analysis. *J Biomol Screen* **11**, 922–932 (2006).

25. Kelm, J. M., Timmins, N. E., Brown, C. J., Fussenegger, M. & Nielsen, L. K. Method for generation of homogeneous multicellular tumor spheroids applicable to a wide variety of cell types. *Biotechnol Bioeng* **83**, 173–180 (2003).

26. Kurosawa, H. Methods for inducing embryoid body formation: in vitro differentiation system of embryonic stem cells. *J Biosci Bioeng* **103**, 389–398 (2007).

27. Kim, J. B. Three-dimensional tissue culture models in cancer biology. *Semin Cancer Biol* **15**, 365–377 (2005).

28. Goodwin, T. J., Prewett, T. L., Wolf, D. A. & Spaulding, G. F. Reduced shear stress: A major component in the ability of mammalian tissues to form three-dimensional assemblies in simulated microgravity. *J Cell Biochem* **51**, 301–311 (1993).

29. Kleinman, H. K. & Martin, G. R. Matrigel: Basement membrane matrix with biological activity. *Semin Cancer Biol* **15**, 378–386 (2005).

30. Tan, W., Krishnaraj, R. & Desai, T. A. Evaluation of Nanostructured Composite Collagen–Chitosan Matrices for Tissue Engineering. *Tissue Engineering* **7**, 203–210 (2001).

31. Grandhi, T. S. P., Potta, T., Nitiyanandan, R., Deshpande, I. & Rege, K. Chemomechanically engineered 3D organotypic platforms of bladder cancer dormancy and reactivation. *Biomaterials* **142**, 171–185 (2017).

32. Alessandri, K. *et al.* Cellular capsules as a tool for multicellular spheroid production and for investigating the mechanics of tumor progression in vitro. *Proc National Acad Sci* **110**, 14843–14848 (2013).

33. Chan, H. F., Zhang, Y. & Leong, K. W. Efficient One-Step Production of Microencapsulated Hepatocyte Spheroids with Enhanced Functions. *Small* **12**, 2720–2730 (2016).

34. Chan, H. F. *et al.* Rapid formation of multicellular spheroids in double-emulsion droplets with controllable microenvironment. *Sci Rep-uk* **3**, 3462 (2013).

35. Williams, S. K., Touroo, J. S., Church, K. H. & Hoying, J. B. Encapsulation of Adipose Stromal Vascular Fraction Cells in Alginate Hydrogel Spheroids Using a Direct-Write Three-Dimensional Printing System. *Bioresearch Open Access* **2**, 448–454 (2013).

36. Lee, K. H. *et al.* Diffusion-mediated in situ alginate encapsulation of cell spheroids using microscale concave well and nanoporous membrane. *Lab Chip* **11**, 1168–1173 (2011).

37. Tostões, R. M. *et al.* Perfusion of 3D encapsulated hepatocytes—A synergistic effect enhancing long-term functionality in bioreactors. *Biotechnol Bioeng* **108**, 41–49 (2011).

38. Massie, I., Selden, C., Hodgson, H. & Fuller, B. Cryopreservation of Encapsulated Liver Spheroids for a Bioartificial Liver: Reducing Latent Cryoinjury Using an Ice Nucleating Agent. *Tissue Eng Part C Methods* **17**, 765–774 (2011).

39. Bhise, N. S. *et al.* A liver-on-a-chip platform with bioprinted hepatic spheroids. *Biofabrication* **8**, 014101 (2016).

40. Katsen-Globa, A., Ehrhart, F., Zimmermann, H., Feilen, P. & Weber, M. M. Alginate encapsulation improves viability and integrity of cryopreserved pancreatic islets and multicellular spheroids: combined fluorescence, scanning and block-face scanning electron microscopy. *Microsc Microanal* **13**, 190–191 (2007).

41. Potta, T. *et al.* Discovery of antibiotics-derived polymers for gene delivery using combinatorial synthesis and cheminformatics modeling. *Biomaterials* **35**, 1977–1988 (2014).

42. Rege, K., Hu, S., Moore, J. A., Dordick, J. S. & Cramer, S. M. Chemoenzymatic Synthesis and High-Throughput Screening of an Aminoglycoside−Polyamine Library: Identification of High-Affinity Displacers and DNA-Binding Ligands. *J Am Chem Soc* **126**, 12306–12315 (2004).

43. Rege, K. *et al.* Investigation of DNA-Binding Properties of an Aminoglycoside-Polyamine Library Using Quantitative Structure−Activity Relationship (QSAR) Models. *J Chem Inf Model* **45**, 1854–1863 (2005).

44. Grandhi, T. S. P. *et al.* Aminoglycoside Antibiotic-Derived Anion-Exchange Microbeads for Plasmid DNA Binding and in Situ DNA Capture. *Acs Appl Mater Inter* **6**, 18577–18589 (2014).

45. Laschke, M. W. & Menger, M. D. Life is 3D: Boosting Spheroid Function for Tissue Engineering. *Trends Biotechnol* **35**, 133–144 (2017).

46. Law, S. & Chaudhuri, S. Mesenchymal stem cell and regenerative medicine: regeneration versus immunomodulatory challenges. 22–38 (2013).

47. Han, H.-W., Asano, S. & Hsu, S. Cellular Spheroids of Mesenchymal Stem Cells and Their Perspectives in Future Healthcare. *Appl Sci* **9**, 627 (2019).

48. Cesarz, Z. & Tamama, K. Spheroid Culture of Mesenchymal Stem Cells. *Stem Cells Int* **2016**, 1–11 (2016).

49. Murphy, K. C., Whitehead, J., Zhou, D., Ho, S. S. & Leach, J. K. Engineering fibrin hydrogels to promote the wound healing potential of mesenchymal stem cell spheroids. *Acta Biomater* **64**, 176–186 (2017).

50. Hsu, S. & Hsieh, P. Self-assembled adult adipose-derived stem cell spheroids combined with biomaterials promote wound healing in a rat skin repair model. *Wound Repair Regen* **23**, 57–64 (2015).

51. Zhang, Q. *et al.* Three-Dimensional Spheroid Culture of Human Gingiva-Derived Mesenchymal Stem Cells Enhances Mitigation of Chemotherapy-Induced Oral Mucositis. *Stem Cells Dev* **21**, 937–947 (2012).

52. Ryu, N.-E., Lee, S.-H. & Park, H. Spheroid Culture System Methods and Applications for Mesenchymal Stem Cells. *Cells* **8**, 1620 (2019).

53. Suenaga, H., Furukawa, K. S., Suzuki, Y., Takato, T. & Ushida, T. Bone regeneration in calvarial defects in a rat model by implantation of human bone marrow-derived mesenchymal stromal cell spheroids. *J Mater Sci Mater Medicine* **26**, 254 (2015).

54. Lee, W.-Y. *et al.* The use of injectable spherically symmetric cell aggregates self-assembled in a thermo-responsive hydrogel for enhanced cell transplantation. *Biomaterials* **30**, 5505–5513 (2009).

55. Tseng, T.-C. & Hsu, S. Substrate-mediated nanoparticle/gene delivery to MSC spheroids and their applications in peripheral nerve regeneration. *Biomaterials* **35**, 2630–2641 (2014).

56. Yamaguchi, Y., Ohno, J., Sato, A., Kido, H. & Fukushima, T. Mesenchymal stem cell spheroids exhibit enhanced in-vitro and in-vivo osteoregenerative potential. *Bmc Biotechnol* **14**, 105 (2014).

57. Tokuyama, H. & Yazaki, N. Preparation of poly(N-isopropylacrylamide) hydrogel beads by circulation polymerization. *React Funct Polym* **70**, 967–971 (2010).

58. Gruškienė, Rūta & Ričardas. Quaternization of chitosan and partial destruction of the quaternized derivatives making them suitable for electrospinning. *Chemija* **24**, 325–334 (2013).

59. Skardal, A., Sarker, S. F., Crabbé, A., Nickerson, C. A. & Prestwich, G. D. The generation of 3-D tissue models based on hyaluronan hydrogel-coated microcarriers within a rotating wall vessel bioreactor. *Biomaterials* **31**, 8426–8435 (2010).

60. Joshi, P. & Lee, M.-Y. High Content Imaging (HCI) on Miniaturized Three-Dimensional (3D) Cell Cultures. *Biosensors* **5**, 768–790 (2015).

61. National Center for Biotechnology Information. PubChem Compound Summary for CID 37768, Amikacin. Retrieved October 15, 2020 from. https://pubchem.ncbi.nlm.nih.gov/compound/Amikacin (2020).

62. Choe, G., Park, J., Park, H. & Lee, J. Y. Hydrogel Biomaterials for Stem Cell Microencapsulation. *Polymers-basel* **10**, 997 (2018).

63. Kim, H. *et al.* Mesenchymal stem cell 3D encapsulation technologies for biomimetic microenvironment in tissue regeneration. *Stem Cell Res Ther* **10**, 51 (2019).

64. Nath, S. & Devi, G. R. Three-dimensional culture systems in cancer research: Focus on tumor spheroid model. *Pharmacol Therapeut* **163**, 94–108 (2016).

65. Darling, D. *et al.* Low-speed centrifugation of retroviral vectors absorbed to a particulate substrate: a highly effective means of enhancing retroviral titre. *Gene Ther* **7**, 914–923 (2000).

66. Ho, Y. K., Zhou, L. H., Tam, K. C. & Too, H. P. Enhanced non-viral gene delivery by coordinated endosomal release and inhibition of β-tubulin deactylase. *Nucleic Acids Res* **45**, e38–e38 (2017).

67. Kühlcke, K. *et al.* Highly Efficient Retroviral Gene Transfer Based on Centrifugation-Mediated Vector Preloading of Tissue Culture Vessels. *Mol Ther* **5**, 473–478 (2002).

68. Pampaloni, F., Reynaud, E. G. & Stelzer, E. H. K. The third dimension bridges the gap between cell culture and live tissue. *Nat Rev Mol Cell Bio* **8**, 839–845 (2007).

69. Patra, B., Peng, C.-C., Liao, W.-H., Lee, C.-H. & Tung, Y.-C. Drug testing and flow cytometry analysis on a large number of uniform sized tumor spheroids using a microfluidic device. *Sci Rep-uk* **6**, 21061 (2016).

70. Givan, A. L. *Flow Cytometry: First Principles*. (n.d.). doi:10.1002/0471223948.

71. Bissell, M. J., Rizki, A. & Mian, I. S. Tissue architecture: the ultimate regulator of breast epithelial function. *Curr Opin Cell Biol* **15**, 753–762 (2003).

72. Weaver, V. M. *et al.* Reversion of the Malignant Phenotype of Human Breast Cells in Three-Dimensional Culture and In Vivo by Integrin Blocking Antibodies. *The Journal of Cell Biology* **137**, 131–145 (1997).